

# Structural optimization of 4-chlorobenzoylpiperidine derivatives for the development of potent, reversible and selective monoacylglycerol lipase (MAGL) inhibitors

*Carlotta Granchi,<sup>†</sup> Flavio Rizzolio,<sup>ϕ</sup> Stefano Palazzolo,<sup>ϕ,§</sup> Sara Carmignani,<sup>†</sup> Marco Macchia,<sup>†</sup> Giuseppe Saccomanni,<sup>†</sup> Clementina Manera,<sup>†</sup> Adriano Martinelli,<sup>†</sup> Filippo Minutolo,<sup>†</sup> Tiziano Tuccinardi<sup>\*†</sup>*

<sup>†</sup> Department of Pharmacy, University of Pisa, Via Bonanno 6, 56126 Pisa, Italy

<sup>ϕ</sup> Division of Experimental and Clinical Pharmacology, Department of Molecular Biology and Translational Research, National Cancer Institute and Center for Molecular Biomedicine, IRCCS, 33081 Aviano (PN), Italy

<sup>§</sup> Graduate School in Nanotechnology, University of Trieste, Trieste, Italy

## ABSTRACT

Monoacylglycerol lipase (MAGL) inhibitors are considered potential therapeutic agents for a variety of pathological conditions, including several types of cancer. Many MAGL inhibitors are reported in literature; however, most of them showed an irreversible mechanism of action, which caused important side effects. The use of reversible MAGL inhibitors has been only partially investigated so far, mainly because of the lack of compounds with good MAGL reversible inhibition properties. In this study, starting from the (4-(4-chlorobenzoyl)piperidin-1-yl)(4-methoxyphenyl)methanone (CL6a) lead compound that showed a reversible mechanism of MAGL inhibition ( $K_i = 8.6 \mu\text{M}$ ), we started its structural optimization and we developed a new potent and selective MAGL inhibitor (**17b**,  $K_i = 0.65 \mu\text{M}$ ). Furthermore, modeling studies suggested that the binding interactions of this compound replace a structural water molecule reproducing its H-bonds in the MAGL binding site, thus identifying a new key anchoring point for the development of new MAGL inhibitors.

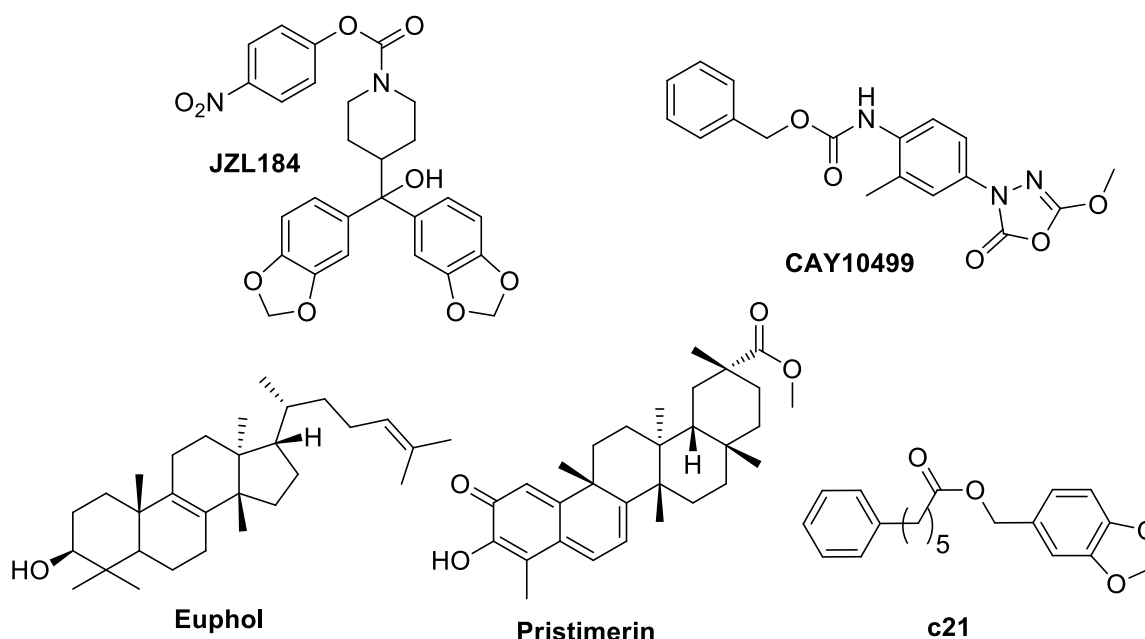
## INTRODUCTION

Among the different endogenous lipids with endocannabinoid-like activity, anandamide (AEA) and 2-arachidonoylglycerol (2-AG) are the two most important endogenous ligands that are able to activate the G protein-coupled cannabinoid receptors, CB<sub>1</sub> and CB<sub>2</sub>.<sup>1</sup> These endocannabinoids are produced on demand through stimulus-dependent cleavage of phospholipid precursors and they modulate multiple physiological processes including pain, inflammation, appetite, memory, and emotion and their signaling functions terminate by enzymatic hydrolysis.<sup>2, 3</sup> In the nervous system, 2-AG is produced by phospholipase C and diacylglycerol lipase and it is deactivated through hydrolysis mediated by monoacylglycerol lipase (MAGL). Because of the prominent role in 2-AG degradation, selective inactivation of MAGL represents a potential target for pharmacological agents able to treat diverse pathological conditions such as cancer, chronic pain and Alzheimer's disease.<sup>4</sup>

In the past ten years, massive efforts have been implemented in order to obtain potent MAGL inhibitors;<sup>5-10</sup> however, almost all the compounds found showed irreversible inhibition properties.<sup>11</sup> In this context the reference inhibitors that have been used in the literature for most cellular and animal experiments are 4-nitrophenyl-4-[bis(1,3-benzodioxol-5-yl)(hydroxy)methyl]piperidine-1-carboxylate **1** (JZL184, Figure 1)<sup>8</sup> and the benzyl(4-(5-methoxy-2-oxo-1,3,4-oxadiazol-3(2*H*)-yl)-2-methylphenyl)carbamate **2** (CAY10499, Figure 1).<sup>5</sup> As reported by Scholsburg and co-workers, the irreversible inhibition of MAGL, induced by repeated administration of **1**, yielded cross-tolerance to CB<sub>1</sub> agonists in mice.<sup>12</sup> Chronic MAGL inhibition also produced physical dependence, desensitized brain CB<sub>1</sub> receptors and damaged endocannabinoid-dependent synaptic plasticity.<sup>12</sup> Genetic inactivation of MAGL or prolonged pharmacological blockage of MAGL by an irreversible inhibitor provokes the persistence of elevated 2-AG levels in the brain. This fact leads to a tolerance of the effects induced by MAGL inhibition. Moreover, responses to CB<sub>1</sub> agonists were significantly reduced and there was an evident cross-tolerance when exogenous CB<sub>1</sub> agonists were administered, resulting in a general CB<sub>1</sub> desensitization. Furthermore, profound alterations to CB<sub>1</sub> receptor expression and function in the brain were observed. Considering all these drawbacks associated to an irreversible MAGL inhibition, the need to discover selective and reversible MAGL inhibitors remains urgent. To our knowledge, the only compounds described as good reversible MAGL inhibitors are the naturally occurring terpenoids **pristimerin** and **euphol** (Figure 1).<sup>13</sup> However, these two compounds act on a large number of secondary targets and this makes their use and study as MAGL inhibitors very difficult.<sup>14,15</sup> Very recently, the reversible MAGL inhibitor benzo[*d*][1,3]dioxol-5-ylmethyl 6-phenylhexanoate **3** (compound c21, Figure 1) was tested *in vivo* using the experimental allergic encephalomyelitis (EAE) mouse model, which is broadly studied as an animal model of human CNS demyelinating diseases, including multiple sclerosis and acute disseminated encephalomyelitis.<sup>16</sup> This molecule was able to ameliorate the clinical progression of the multiple sclerosis mouse model and, very importantly, the therapeutic effects were not accompanied by catalepsy or other motor

impairments that have been observed after the administration of irreversible MAGL inhibitors, thus supporting the hypothesis that reversible inhibitors could be profitably used in *in vivo* models.<sup>16</sup>

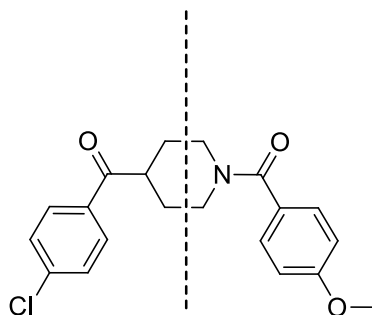
We have recently reported a virtual screening study for the discovery of new reversible MAGL inhibitors. Among the tested compounds, (4-(4-chlorobenzoyl)piperidin-1-yl)(4-methoxyphenyl)methanone **4** (CL6a, Figure 2) proved to be an interesting reversible MAGL inhibitor lead due to its inhibition activity ( $K_i = 8.6 \mu\text{M}$  and  $\text{IC}_{50} = 11.7 \mu\text{M}$ ), the absence of stereocenters in its structure and its good synthetic accessibility.<sup>17</sup> With the aim of identifying potent and selective MAGL inhibitors, chemical modifications guided by molecular modeling predictions of the probable binding poses were made to the structure of the initial compound **4** as a first step of our attempt to improve the inhibition potency of **4** on MAGL. The synthesis of new analogues of **4**, their biological characterization on the isolated enzyme as well as their antiproliferative activities on a series of cancer cells are reported in this study.



**Figure 1.** Structures of known MAGL inhibitors.

## RESULTS AND DISCUSSION

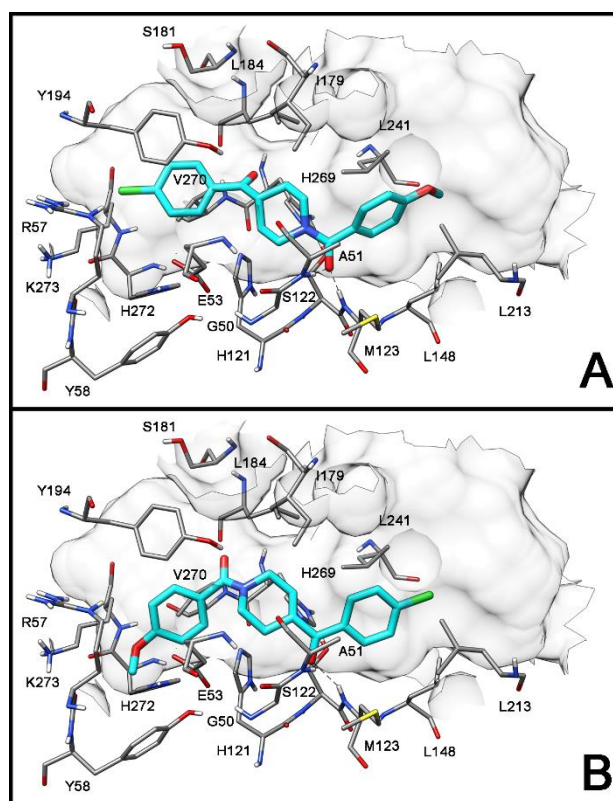
**Design and Molecular Modeling.** As shown in Figure 2, by using a plane that divides the piperidine ring we can observe that compound **4** is symmetrical, with the exception of the piperidine nitrogen atom and the different aryl substituents at the two opposite sides of the molecule (a chloro atom in position 4 of the phenyl ring of the ketone side and a methoxy group in the same position of the phenyl ring of the amidic portion).



**Figure 2.** 2D analysis of compound **4**.

Before proceeding with the synthesis of **4** analogues, an extensive docking analysis was carried out in order to establish the binding disposition of this ligand. Figure S1 shows the clustering analysis of the docking results. This plot highlights the presence of two possible binding dispositions of the ligand, as there are two highly populated clusters of docking poses with very similar energy interaction scoring values. The most energetically favorable binding mode shows that the amidic C=O group of **4** forms two H-bonds with the nitrogen backbone of A51 and M123 and the 4-methoxyphenyl fragment is directed towards an open cavity of the protein showing lipophilic interactions with L148, L213 and L241. The 4-chlorobenzoyl moiety is inserted into a small pocket of the protein and shows lipophilic interactions of the phenyl ring with Y194 and V270 (binding mode A of Figure 3). Figure 3B shows a representative docking pose of the second cluster which is more populated than the first one, but it shows a slightly lower energy interaction score. As expected, this binding disposition is symmetrical to the first one: the 4-chlorobenzoyl moiety of the **4** is directed towards the open cavity of the protein showing lipophilic interactions with L148, L213 and L241 and

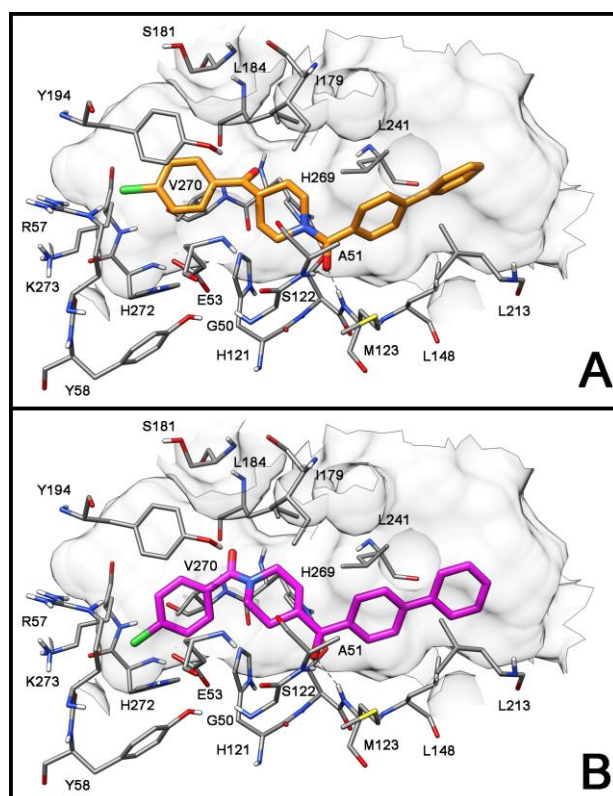
forms two H-bonds with the nitrogen backbone of A51 and M123. With regards to the 4-methoxybenzoyl fragment, it is inserted into the small pocket of the protein and the phenyl ring shows lipophilic interactions with Y194 and V270.



**Figure 3.** Docking of compound **4** into *hMAGL*. (A) Binding mode A; (B) binding mode B.

In order to identify which one is the preferred binding mode among the two proposed solutions by the docking analysis (see Figure 3), we planned to synthesize two analogues of compound **4** that are respectively able to adopt only one of these binding modes. In fact, biphenylic compounds **5** and **6** (Table 1) were designed considering: a) the small volume of the pocket delimited by E53, R57, Y58, Y194, V270 and H272, and b) the open shape of the cavity on the opposite side of the binding site. These two compounds are characterized by the presence of a bulky biphenyl ring that we hypothesized could lie only in the open cavity of the binding site surrounded by hydrophobic residues L148, L213 and L241. As shown in Figure 4 and Figure S2, our hypothesis was confirmed by the

docking studies, since there was only one predicted binding disposition for each compound, with the biphenyl ring that was placed in the open cavity of the binding site. Due to this disposition, compound **5** shows the binding mode A, with the C=O amidic group forming two H-bonds with the backbone N-H of A51 and M123. Conversely, compound **6** shows the binding mode B, with the ketone group that forms two H-bonds with the backbone nitrogen of A51 and M123.

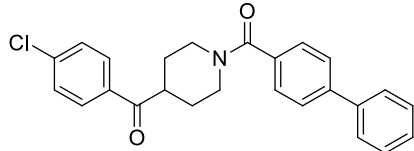
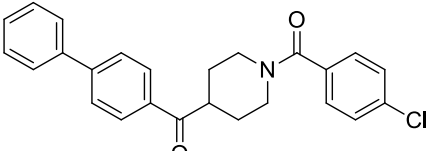
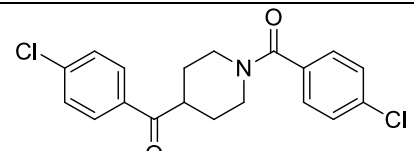
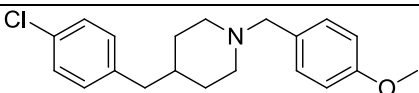
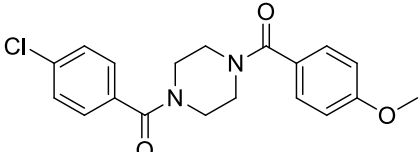


**Figure 4.** Docking results of compound **5** (A) and **6** (B) into *hMAGL*.

The two compounds were thus synthesized and tested for their *hMAGL* inhibition activity together with the piperidine-1,4-diylbis((4-chlorophenyl)methanone) derivative (**7a**, Table 1), which was used as a reference compound, since it possesses the *para*-chloro substituted phenyl ring on both sides of the molecule, without the bulky biphenyl part that is present in the amidic portion of compound **5** or in the ketone moiety of compound **6**. As shown in Table 1, in agreement with the docking results,

both binding modes are possible since both compounds show inhibition of MAGL activity. However, the binding mode B is the preferred one, since compound **6** shows a 5-fold higher activity ( $IC_{50} = 2.1 \mu M$ ) than that of compound **5** ( $IC_{50} = 9.9 \mu M$ ). Subsequently, two derivatives of compound **4** were synthesized and tested for their *h*MAGL inhibition activity in order to inspect the role of the central scaffold (Table 1). Compound **8**, which is characterized by the replacement of the two C=O groups with two methylene moieties, showed a complete loss of inhibition activity ( $IC_{50}$  greater than  $100 \mu M$ ). Similar results were also obtained for compound **9**, which possesses a central piperazine ring instead of piperidine, thus introducing a second amidic group that further rigidifies the structure by reducing the rotational freedom of the *p*-chlorobenzoyl portion. Both results supported the important role of the central piperidine ring bearing a carbonyl group in the opposite position to the amidic fragment for the establishment of an efficient interaction with the enzyme, thus confirming the key role played by the central scaffold of **4**, which justifies the development of a series of analogues of this compound.

**Table 1.** Structure and *h*MAGL activity of compounds **5**, **6**, **7a**, **8** and **9**.

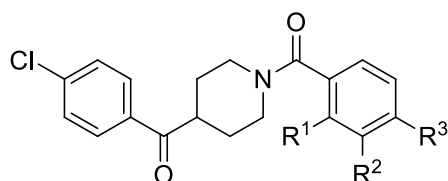
| #         | Structure   | $IC_{50}$ ( $\mu M$ ) |
|-----------|---|-----------------------|
| <b>5</b>  |  | $9.9 \pm 0.6$         |
| <b>6</b>  |  | $2.1 \pm 0.4$         |
| <b>7a</b> |  | $5.4 \pm 0.1$         |
| <b>8</b>  |  | $> 100$               |
| <b>9</b>  |  | $> 100$               |



Hence, once we identified the preferred binding mode of this class of compounds into *h*MAGL, we proceeded with the lead optimization of **4**. As a first step in the development of this scaffold, we decided to improve the interaction of the compound inside the small pocket delimited by E53, R57, Y58, Y194, V270 and H272 while maintaining the rest of the molecule fixed. On this basis, we replaced the *p*-methoxyphenyl ring present in the amidic portion of the initial compound **4** with differently substituted aryl groups and kept the *p*-chlorobenzoyl unit fixed. Hence, we explored the *ortho/meta/para* effects generated by the presence in the amidic phenyl ring of halogen atoms (F, Cl, Br, I), methyl, trifluoromethyl, methoxy, trifluoromethoxy, hydroxy, amino and nitro substituents, by testing the inhibitory activities of the series of novel compounds reported in Table 2.

**Enzymatic experiments.** The inhibitory effects of the newly synthesized compounds on human isoforms of MAGL by using 4-nitrophenylacetate substrate are reported in Table 2, together with those of the reference irreversible inhibitor **1** and of the recently reported reversible inhibitor **3**. Considering the activity of compound **20** ( $IC_{50} = 6.5 \mu M$ ), which possesses an unsubstituted phenyl ring, the introduction in all the three *o/m/p* positions of the aromatic ring of bromine and iodine (compounds **11a-c** and **12a-c**) determined an increase of the activity ( $IC_{50}$  values in the range 2.4-4.8  $\mu M$ ). The presence of the other substituents generally led to a certain reduction of inhibition activity, which resulted to be either lower than that of reference compound **20** ( $IC_{50}$  values in the range 9.9-57.3  $\mu M$ ) or comparable ( $IC_{50} = 5.4 \mu M$  for **7a**,  $IC_{50} = 7.1 \mu M$  for **13c**). It is worth noting that almost all the reported compounds show an activity that is similar or even better than that of the reference reversible inhibitor **3**.

**Table 2.** Structures and *h*MAGL inhibitory activities of the synthesized compounds.



| Compounds  | R <sup>1</sup>   | R <sup>2</sup>   | R <sup>3</sup>   | IC <sub>50</sub> (μM) |
|------------|------------------|------------------|------------------|-----------------------|
| <b>7a</b>  | H                | H                | Cl               | 5.4 ± 0.7             |
| <b>7b</b>  | H                | Cl               | H                | 17.1 ± 0.1            |
| <b>7c</b>  | Cl               | H                | H                | 10.4 ± 0.5            |
| <b>10a</b> | H                | H                | F                | 17.8 ± 0.9            |
| <b>10b</b> | H                | F                | H                | 20.4 ± 0.1            |
| <b>10c</b> | F                | H                | H                | 13.4 ± 0.6            |
| <b>11a</b> | H                | H                | Br               | 2.4 ± 0.1             |
| <b>11b</b> | H                | Br               | H                | 4.8 ± 0.4             |
| <b>11c</b> | Br               | H                | H                | 4.0 ± 0.4             |
| <b>12a</b> | H                | H                | I                | 4.4 ± 0.2             |
| <b>12b</b> | H                | I                | H                | 4.3 ± 0.4             |
| <b>12c</b> | I                | H                | H                | 2.4 ± 0.2             |
| <b>13a</b> | H                | H                | CH <sub>3</sub>  | 11.8 ± 0.4            |
| <b>13b</b> | H                | CH <sub>3</sub>  | H                | 10.9 ± 0.8            |
| <b>13c</b> | CH <sub>3</sub>  | H                | H                | 7.1 ± 0.1             |
| <b>14a</b> | H                | H                | CF <sub>3</sub>  | 29.8 ± 1.3            |
| <b>14b</b> | H                | CF <sub>3</sub>  | H                | 11.9 ± 0.4            |
| <b>14c</b> | CF <sub>3</sub>  | H                | H                | 26.3 ± 2.4            |
| <b>4</b>   | H                | H                | OCH <sub>3</sub> | 11.7 ± 2.2            |
| <b>15b</b> | H                | OCH <sub>3</sub> | H                | 9.9 ± 1.7             |
| <b>15c</b> | OCH <sub>3</sub> | H                | H                | 11.5 ± 0.3            |
| <b>16a</b> | H                | H                | OCF <sub>3</sub> | 26.6 ± 2.6            |
| <b>16b</b> | H                | OCF <sub>3</sub> | H                | 16.3 ± 1.0            |
| <b>16c</b> | OCF <sub>3</sub> | H                | H                | 17.3 ± 1.2            |
| <b>17a</b> | H                | H                | OH               | 11.7 ± 1.7            |
| <b>17b</b> | H                | OH               | H                | 0.84 ± 0.04           |
| <b>17c</b> | OH               | H                | H                | 32.8 ± 4.3            |
| <b>18a</b> | H                | H                | NH <sub>2</sub>  | 16.7 ± 1.7            |
| <b>18b</b> | H                | NH <sub>2</sub>  | H                | 57.3 ± 2.2            |
| <b>18c</b> | NH <sub>2</sub>  | H                | H                | 15.5 ± 1.9            |
| <b>19a</b> | H                | H                | NO <sub>2</sub>  | 14.2 ± 0.3            |
| <b>19b</b> | H                | NO <sub>2</sub>  | H                | 24.9 ± 3.5            |
| <b>19c</b> | NO <sub>2</sub>  | H                | H                | 24.0 ± 0.4            |
| <b>20</b>  | H                | H                | H                | 6.5 ± 0.1             |
| <b>1</b>   |                  |                  |                  | 0.048 ± 0.005         |
| <b>2</b>   |                  |                  |                  | 0.134 ± 0.015         |
| <b>3</b>   |                  |                  |                  | 9.0 ± 1.5             |

Among the 34 reported derivatives, the *m*-hydroxy-substituted derivative **17b** showed a high inhibition activity (IC<sub>50</sub> = 0.84 μM), about 14 fold more potent than the starting **4** lead compound. In order to better rationalize the activity of this compound, **17b** was subjected to docking calculations,

together with its analogues **17a** and **17c**. Binding mode B of compound **17b** resulted to be more energetically favorable than the other one (see Figure S3). The overall disposition of the molecule is comparable to that observed for compound **4**, with the 4-chlorobenzoyl moiety that is directed towards the open cavity of the protein showing lipophilic interactions with L148, L213 and L241 and the formation of two H-bonds with the backbone nitrogen of A51 and M123 (see Figure 5). The *m*-hydroxybenzoyl fragment is inserted into the small pocket of the protein and shows lipophilic interactions between its aryl ring and residues Y194 and V270. Furthermore, the *m*-hydroxyl participates to a highly energetic H-bond network with residues E53 and H272, where it behaves as a H-bond acceptor with H272 and as a H-bond donor with E53. It is interesting to note that, analyzing the main crystal structures of *h*MAGL<sup>18-21</sup> and superimposing them with the *h*MAGL-**17b** complex, the hydroxyl group of the ligand replaces a structural water molecule that acts as a H-bond bridge between E53 and H272, thus supporting the high activity of this compound (see Figure S4). The replacement of the *m*-hydroxyl with the *o*- and *p*-hydroxyl group determined a marked decrease of the MAGL inhibition activity (see compounds **17c** and **17a**, respectively). As shown in Figure S5, the docking results suggested that for both compounds the shift of the hydroxyl group from the *meta* to *para* and *ortho* position determines the loss of the H-bonds with E53 and H272, without establishing any further interaction.

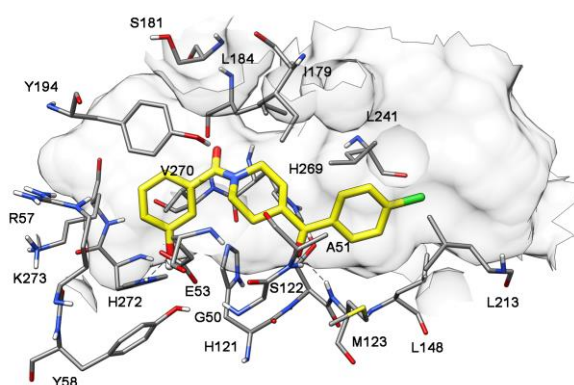


**Figure 5.** Docking results of compound **17b** into *h*MAGL.

The replacement of the *m*-hydroxy with the *m*-amine group led to a marked decrease of activity (compound **18b**,  $IC_{50} = 57.3 \mu\text{M}$ ). Due to the planar geometry of the aniline nitrogen atom and to the delocalization of its electron lone pair in the adjacent  $\pi$ -system, it is unlikely that this group is able to act as a H-bond acceptor, thus supporting the low activity of this compound.

With the aim of evaluating the reversible or irreversible mechanism of inhibition, the effects of dilution and preincubation on the inhibitory ability of compound **17b** and of reference compounds **2** and **3** were evaluated. In the dilution experiments, if the compound is an irreversible inhibitor, then its inhibition potency should not drop upon dilution, whereas inhibition levels should be substantially reduced upon dilution in the presence of a reversible inhibitor. As shown in Figure 6, **17b** showed reversible inhibition, since the inhibition produced by 20  $\mu\text{M}$  of the compound was significantly higher compared with that observed with a 40X dilution, which appears similar to that produced by a 0.5  $\mu\text{M}$  concentration of the compound. The same results were also obtained for compound **3**, whereas compound **2** showed an irreversible inhibition since the inhibition produced by 4  $\mu\text{M}$  of the compound was substantially unchanged upon a 40X dilution, which appears significantly higher to that produced by a 0.1  $\mu\text{M}$  concentration of this compound.

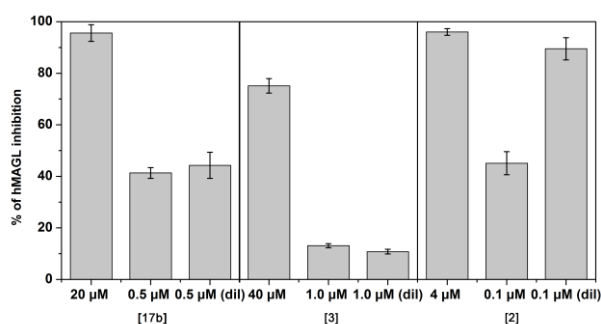


**Figure 6.** Dilution assay for compounds **17b**, **3** and **2**: the first two columns indicate the inhibition percentage of compounds at a concentration of 20  $\mu\text{M}$  and 0.5  $\mu\text{M}$  (**17b**), 40  $\mu\text{M}$  and 1.0  $\mu\text{M}$  (**3**) and

4  $\mu\text{M}$  and 0.1  $\mu\text{M}$  (**2**). The third column indicates the inhibition percentage of compounds after a 40X dilution (final concentration = 0.5  $\mu\text{M}$ , 1.0  $\mu\text{M}$  and 0.1  $\mu\text{M}$  for compounds **17b**, **3** and **2**, respectively).

In order to further support these results, the activity of **17b**, **2** and **3** were tested at different preincubation times of the inhibitors with the enzyme. An irreversible inhibitor will increase its ability to block MAGL over gradually longer incubation times. On the contrary, unchanged  $\text{IC}_{50}$  values in these experiments support a reversible mechanism of action.<sup>22</sup> As expected, compound **17b** and **3** showed a constant MAGL inhibition activity even after 60 min of preincubation, thus supporting a reversible mode of action (see Figure 7). As expected, instead, a time-dependent increase of potency was observed for reference compound **2**, which further supports its already known irreversible inhibitor character.<sup>5</sup>

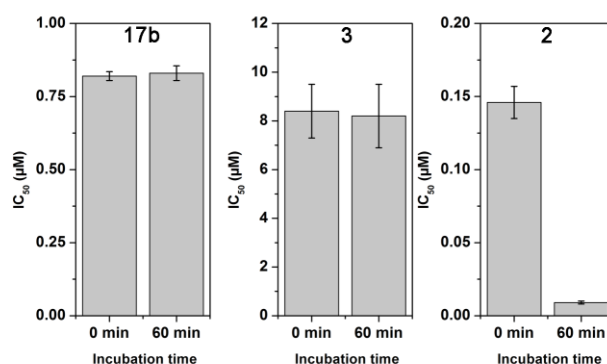


**Figure 7.**  $\text{IC}_{50}$  ( $\mu\text{M}$ ) values of **17b**, **3** and **2** at different preincubation times with *h*MAGL (0 min and 60 min).

Once we confirmed the reversibility of the inhibitory action of compound **17b**, we then evaluated its inhibition mode by measuring Michaelis–Menten kinetics. The dataset was plotted as substrate concentration *versus* enzyme activity and analyzed by applying the mixed-model inhibition fit of

GraphPad Prism 5.0. This model, beyond the  $V_{\max}$  and  $K_m$  values, also calculates the  $\alpha$  parameter, which can be useful for establishing the inhibition mechanism. Its value is greater than zero and determines the extent to which the binding process of the inhibitor changes the affinity of the enzyme for the substrate. If the inhibitor does not modify the binding of the substrate to the enzyme,  $\alpha$  is equal to one and the mixed-model corresponds to a noncompetitive inhibition. When  $\alpha$  is a very large value, the binding of the inhibitor prevents that of the substrate and the mixed-model corresponds to a competitive inhibition. Finally, when  $\alpha$  is a very small value, the binding of the inhibitor increases the binding of the substrate to the enzyme, and the mixed-model corresponds to an uncompetitive model. Kinetic studies indicate for **17b** a  $K_i$  value of  $0.65 \pm 0.05 \mu\text{M}$  and an  $\alpha$  value greater than 10000, thus suggesting a competitive binding for this compound (Figure 8).

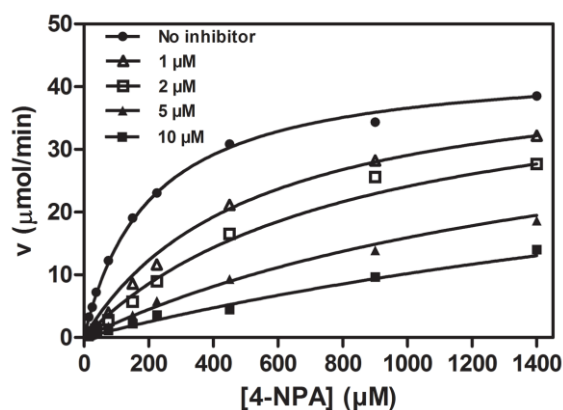


**Figure 8.** Michaelis–Menten plot for the determination of the  $K_i$  of compound **17b** for *hMAGL* ( $K_i = 0.65 \pm 0.05 \mu\text{M}$ ,  $\alpha > 10000$ ).

As a further analysis, in order to explore the potential activity of these compounds for other hydrolases, the selectivity *versus* the analogue enzyme fatty acid amide hydrolase (FAAH) of some of the most promising inhibitors was evaluated. As shown in Table 4, all the tested compounds

showed MAGL selectivity. In particular, compound **17b** displayed a MAGL selectivity greater than 119-fold.

**Table 4.** MAGL selectivity *versus* FAAH for the best compounds.

| Compd      | MAGL IC <sub>50</sub> (μM) | FAAH IC <sub>50</sub> (μM) | Selectivity Index |
|------------|----------------------------|----------------------------|-------------------|
| <b>11b</b> | 4.8 ± 0.4                  | > 100                      | > 21              |
| <b>12c</b> | 2.4 ± 0.2                  | 86.7 ± 5.1                 | 36                |
| <b>13c</b> | 7.1 ± 0.2                  | > 100                      | > 14              |
| <b>17b</b> | 0.84 ± 0.04                | > 100                      | > 119             |
| <b>3</b>   | 9.0 ± 1.5                  | 27.7 ± 1.1                 | 3                 |

**Molecular dynamic simulation.** In order to evaluate the reliability of the docking results and to carry out an analysis of the ligand–protein interaction, the *h*MAGL-**17b** complex was used as a starting structure for 51 ns of molecular dynamic (MD) simulation. As shown in Figure S6, the complex is stable during the simulations and the analysis of the root-mean-square deviation (rmsd) of all the heavy atoms from the X-ray structures highlights a stabilization of the rmsd value around 0.8 Å. With regard to the geometry of the compounds, analyzing the rmsd of the position of the ligand during the simulations with respect to the starting structure, it maintains its starting disposition with an rmsd value between 0.3 and 0.7 Å. With regard to the H-bond analysis (Table S1 in the Supporting Information), the interaction of the hydroxyl group with E53 and H272 appears to be very stable, similarly to the interaction with the nitrogen backbone of A51. Differently from what reported in the docking studies, the interaction with the backbone nitrogen of M123 is not highly conserved; however, this is due to a small shift of the ligand with the formation of a very stable H-bond between the hydroxyl group of S181 and the amidic oxygen of the compound (see Figure S7).

**Antiproliferative assays.** Compound **17b** was also further tested in *in vitro* experiments for evaluating its antiproliferative activity against cancer cells. Compound **2** and **3** were used as reference compounds. Due to the potential role of MAGL as a therapeutic target in ovarian cancer,<sup>23</sup> four human ovarian cancer cell lines (OVSAHO, OVCAR3, COV318 and CAO3) were chosen and a western blot analysis was carried out in order to measure the overexpression of MAGL in these cells. As shown in Figure 9A, western blot analysis highlighted an overexpression of MAGL in OVCAR3 and CAO3 compared to OVSAHO and COV318 cell lines. Compound **17b** caused a considerable inhibition of cell viability, with IC<sub>50</sub> values ranging from 31.5 to 43.9 μM in the OVCAR3 and CAO3 cell lines (Table S2), whereas it proved to be remarkably less potent against ovarian cancer cells that do not overexpress MAGL, such as OVSAHO and COV318 cells. Furthermore, **17b** proved to be completely inactive also against noncancerous human fibroblast lung cells (MRC5, Figure 9B). Differently, the covalent reference inhibitor **2** showed inhibition of cell viability in all the four ovarian cancer cell lines, with IC<sub>50</sub> values ranging from 17.2 to 83.1 μM (Table S2). This behavior may be due to the lack of target-selectivity of this compound, thus we cannot exclude that the involvement of different targets could contribute to its antiproliferative potential. Surprisingly, the known MAGL inhibitor **3** displayed a substantial inactivity against all the tested cell lines. Overall, these data suggest that the reversible inhibition of MAGL operated by the herein reported class of compounds may be a possible profitable alternative to the irreversible inhibition treatment.



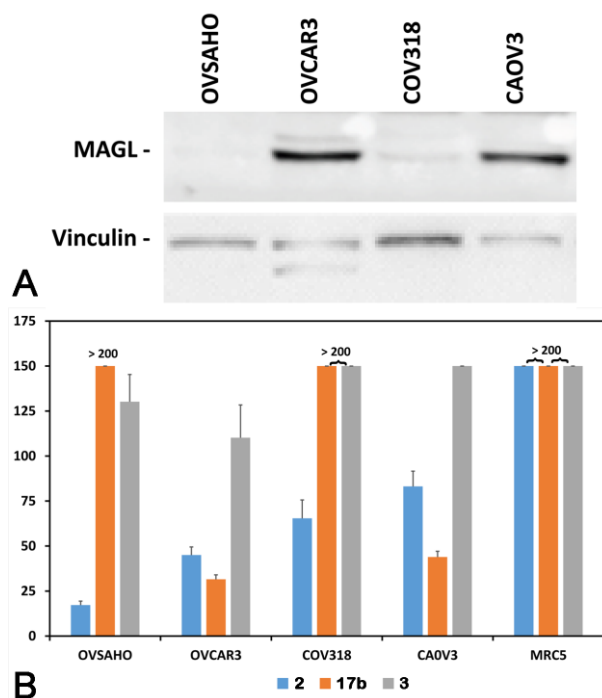
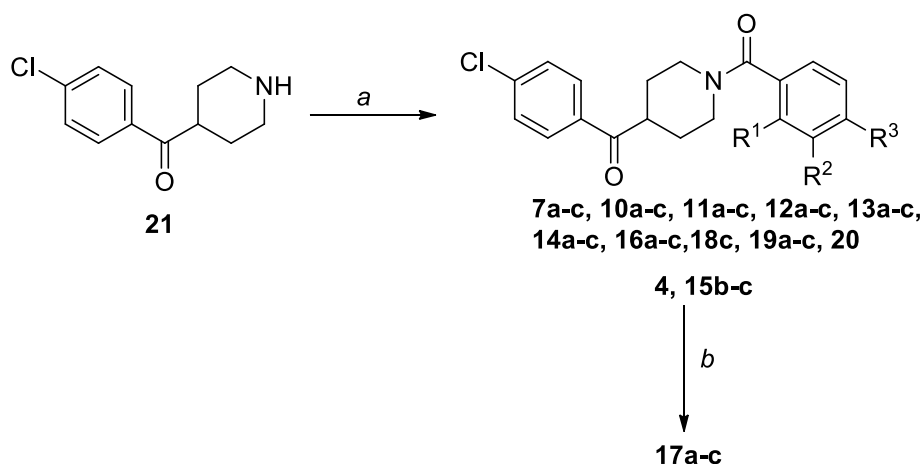


**Figure 9.** A) Western blot analysis of MAGL expression in ovarian cancer cell lines. Vinculin was utilized to normalize the amount of total loaded proteins. B) Cell growth inhibitory activities (IC<sub>50</sub>) of compounds **2**, **17b** and **3**.

**Chemistry.** Benzoyl piperidine derivatives **4**, **7a-c**, **10a-c**, **11a-c**, **12a-c**, **13a-c**, **14a-c**, **15b-c**, **16a-c**, **19a-c** and **20** were synthesized by an amide coupling between properly substituted benzoic acids and 4-(4-chlorobenzoyl)piperidine **21** in the presence of the condensing agent HATU and DIPEA as the base in dry *N,N*-dimethylformamide as the solvent, as previously reported for compound **4**.<sup>17</sup> Hydroxy-substituted derivatives **17a-c** were obtained after BBr<sub>3</sub>-promoted deprotection of the corresponding methoxylated precursors **4**, **15b-c**. A particular case was the *ortho*-amino substituted compound **18c** which, unlike its analogues *para*- and *meta*-NH<sub>2</sub>-bearing compounds **18a-b** (see Scheme 2), was directly obtained from condensation of 4-(4-chlorobenzoyl)piperidine with anthranilic acid (Scheme 1), since the protection of the amino moiety with *tert*-butyloxycarbonyl group, similarly adopted for the *para*- and *meta*-analogues, needed very long reaction times with the

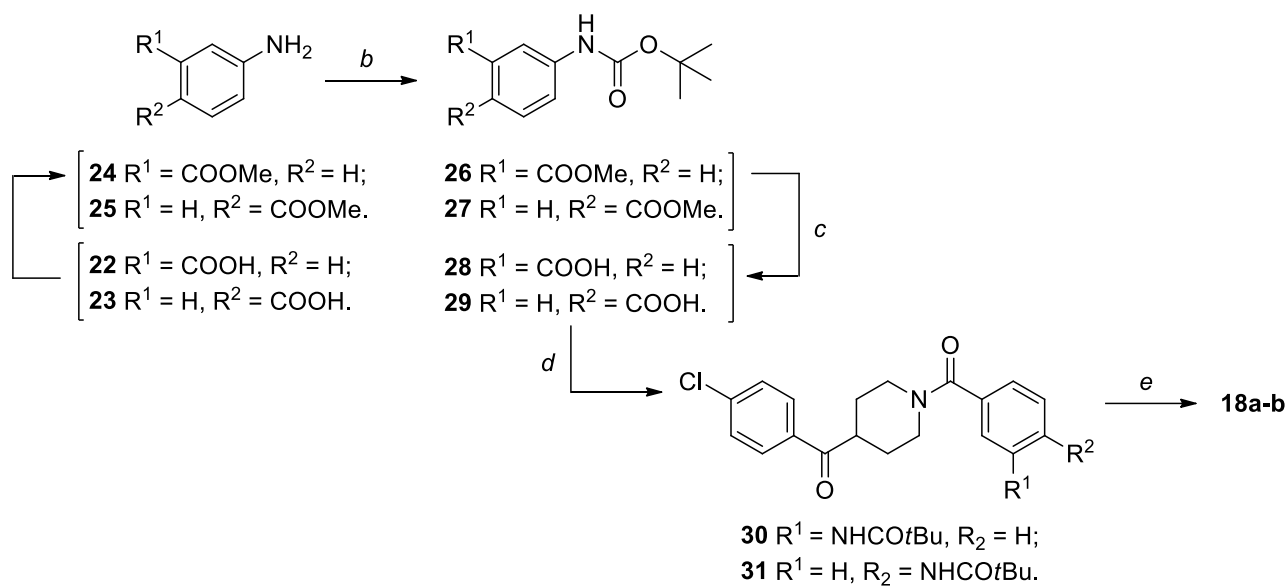
simultaneous formation of many side-products, therefore the direct condensation was preferred, although this caused a decrease in the reaction yield.



### Scheme 1. Synthesis of benzoyl-piperidine derivatives.<sup>a</sup>

<sup>a</sup>Reagents and conditions: (a) properly substituted benzoic acid (1 eq), HATU (1.05 eq), DIPEA (4 eq), dry DMF, RT, 6-8 h; (b) 1M BBr<sub>3</sub>, dry CH<sub>2</sub>Cl<sub>2</sub>, -78 to 0 °C, then RT, 1-2 h.

As anticipated in the previous discussion, the synthesis of amino-substituted compounds **18a-b** started with the formation of the methyl esters **24** and **25** from the corresponding amino-benzoic acids **22** and **23** by refluxing them in MeOH in the presence of SOCl<sub>2</sub> (Scheme 2). Boc-protection of the amino groups with di-*tert*-butyl dicarbonate in the presence of triethylamine in THF gave compounds **26** and **27**, which were then hydrolyzed to give Boc-protected benzoic acids **28** and **29** ready to be condensed with piperidine **21**. The amino groups of the intermediate amides **30** and **31** were finally deprotected by reaction with trifluoroacetic acid in DCM to obtain compounds **18a** and **18b** in good yields.

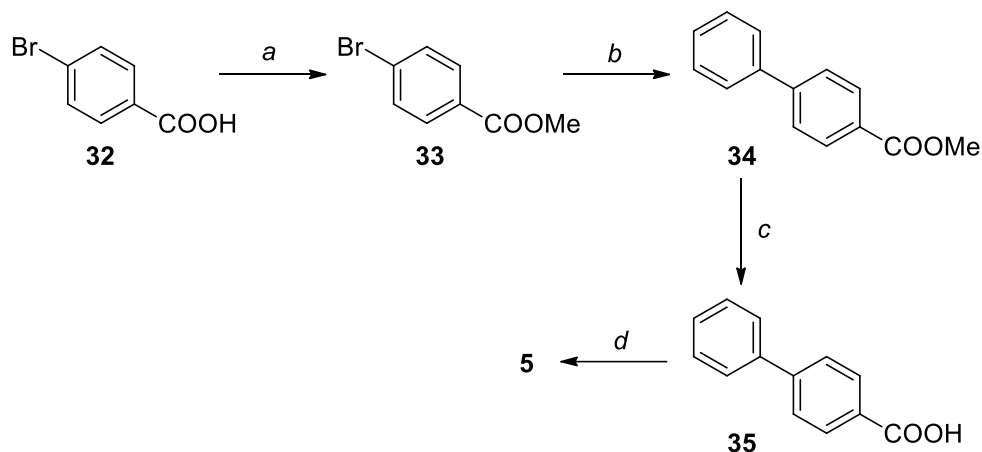


**Scheme 2. Synthesis of *meta* and *para*-amino-substituted benzoyl-piperidine derivatives 18a-b.<sup>a</sup>**

<sup>a</sup>Reagents and conditions: *a*) MeOH, SOCl<sub>2</sub> (2.5 eq), reflux, 3 h; *b*) (Boc)<sub>2</sub>O (2 eq), Et<sub>3</sub>N (2 eq), dry THF, RT, 24 h; *c*) aq. 2N LiOH (6 eq), THF/MeOH 1:1 v/v, RT, overnight; *d*) (4-chlorophenyl)(piperidin-4-yl)methanone **21** (1 eq), HATU (1.05 eq), DIPEA (4 eq), dry DMF, RT, 3-4 h; *e*) CF<sub>3</sub>COOH, dry DCM, 0 °C to RT, 3-5 h.

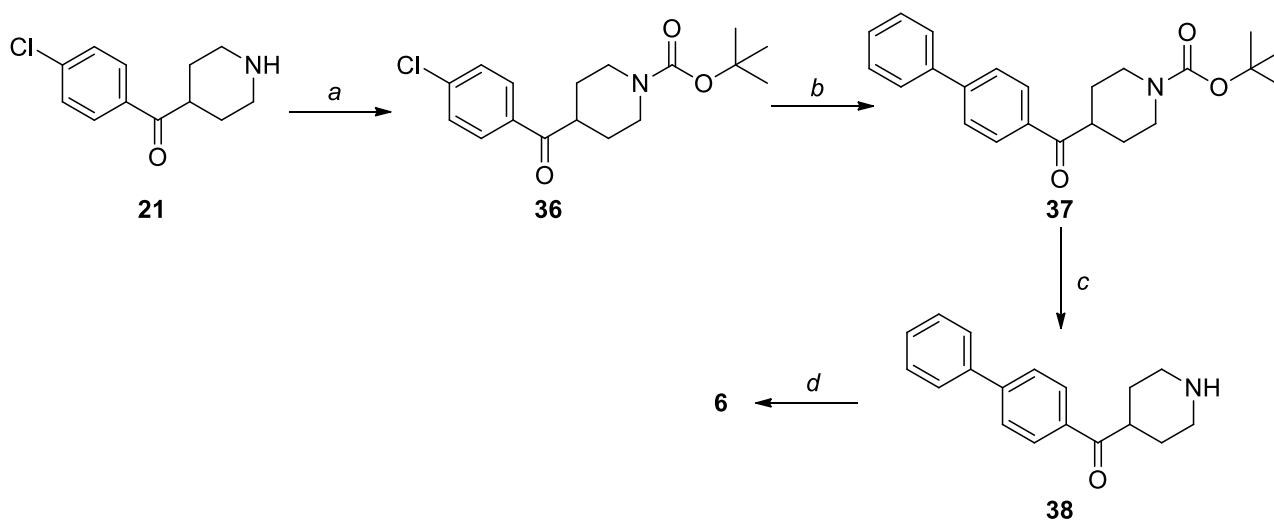
The synthetic approaches for the synthesis of the biphenyl derivatives **5** and **6** are reported in Schemes 3 and 4. For the synthesis of compound **5**, [1,1'-biphenyl]-4-carboxylic acid **35** was obtained after a sequence of reactions starting from 4-bromobenzoic acid **32**, consisting in a Fischer esterification to obtain the methyl ester **33**, followed by a palladium-catalyzed cross-coupling reaction to replace the bromine atom with a phenyl ring. This step required anhydrous conditions to prevent the hydrolysis of the methyl ester group under prolonged heating in the presence of alkaline solutions, since the isolation and purification of the biphenyl methyl ester was preferred. Finally, hydrolysis of the methyl ester gave compound **35** which was condensed with 4-(4-chlorobenzoyl)piperidine **21** in the presence of HATU and DIPEA to yield the desired compound. The synthesis of compound **6** started with the protection of piperidine **21**, then a cross-coupling reaction adopting the Fu-type conditions, which are suitable for the coupling of aryl chlorides with the appropriate phenylboronic acid, using the catalytic

system containing Pd<sub>2</sub>(dba)<sub>3</sub> and tricyclohexylphosphine, and cesium carbonate as the base, gave compound **37**. TFA-promoted deprotection of the piperidine *N*-atom gave compound **38**, which was reacted with 4-chlorobenzoic acid in the same conditions adopted for all the amidic condensation of this class of compounds to produce compound **6** in high yields.



### Scheme 3. Synthesis of biphenyl derivative **5**.<sup>a</sup>

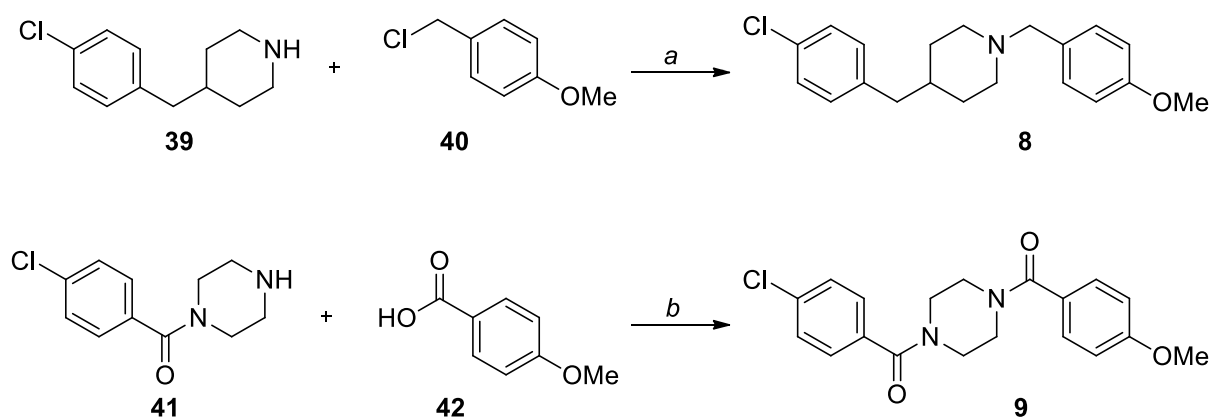
<sup>a</sup>Reagents and conditions: (a) MeOH, H<sub>2</sub>SO<sub>4</sub>, reflux, overnight; (b) PhB(OH)<sub>2</sub> (2 equiv), Pd(OAc)<sub>2</sub> (0.03 eq), PPh<sub>3</sub> (0.15 eq), K<sub>2</sub>CO<sub>3</sub> (1.5 eq), toluene, 100 °C, 18 h; (c) aq. 2N LiOH (6 eq), THF/MeOH 1:1 v/v, RT, 20 h; (d) (4-chlorophenyl)(piperidin-4-yl)methanone **21** (1 eq), HATU (1.05 eq), DIPEA (4 eq), dry DMF, RT, 3 h.



### Scheme 4. Synthesis of biphenyl derivative **6**.<sup>a</sup>

<sup>a</sup>Reagents and conditions: (a) (Boc)<sub>2</sub>O (1.2 eq), Et<sub>3</sub>N (2 eq), dry THF, RT, 2 h; (b) PhB(OH)<sub>2</sub> (1.6 equiv), Pd<sub>2</sub>(dba)<sub>3</sub> (0.032 eq), Cy<sub>3</sub>P 20% toluene (0.08 eq), Cs<sub>2</sub>CO<sub>3</sub> (1.7 eq), dioxane, 100 °C, overnight; (c) CF<sub>3</sub>COOH, dry DCM, 0 °C to RT, 2 h; (d) 4-chlorobenzoic acid (1 eq), HATU (1.05 eq), DIPEA (4 eq), dry DMF, RT, 6 h.

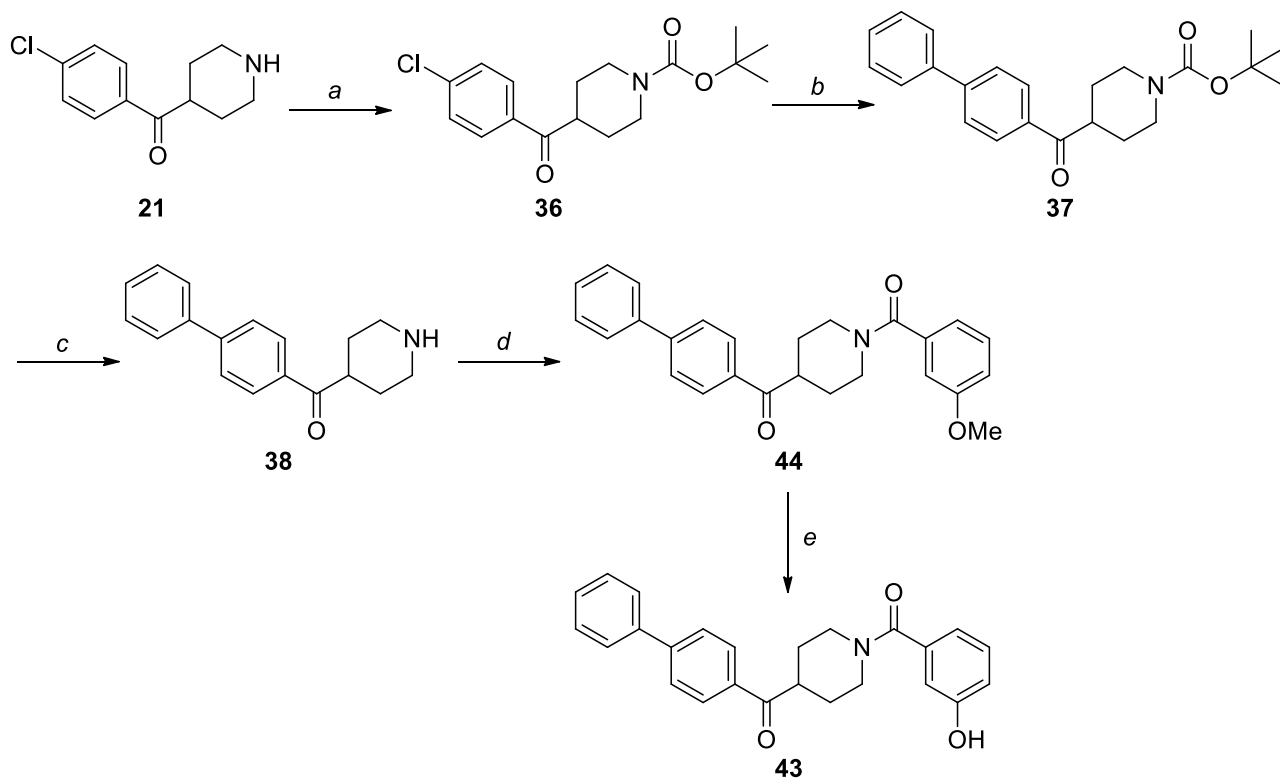
The synthesis of compounds **8** and **9** is reported in Scheme 5 and for both derivatives a one-pot procedure gave the desired products. Derivative **8** was obtained by alkylation of 4-(4-chlorobenzyl)piperidine hydrochloride **39** with 4-methoxybenzyl chloride **40** using potassium carbonate as the base. Differently, the amidic condensation between 1-(4-chlorobenzoyl)piperazine **41** and 4-methoxybenzoic acid **42** under the same conditions previously described for the synthesis of other compounds (Schemes 1-4) gave derivative **9**.



#### Scheme 5. Synthesis of compounds **8** and **9**.<sup>a</sup>

<sup>a</sup>Reagents and conditions: (a) an. K<sub>2</sub>CO<sub>3</sub> (3 eq.), dry DMF, RT, overnight; (b) HATU (1.05 eq), DIPEA (4 eq), dry DMF, RT, 3 h.

For the synthesis of compound **43** (see Conclusions section), the synthetic scheme described for the preparation of biphenylic piperidine **38** (Scheme 4) was adopted, then piperidine **38** was submitted to a condensation with 3-methoxybenzoic acid to get amide **44**, followed by deprotection of the methoxy group with boron tribromide, to obtain the final compound **43** (Scheme 6).



### Scheme 6. Synthesis of compound 43.<sup>a</sup>

<sup>a</sup>Reagents and conditions: (a) (Boc)<sub>2</sub>O (1.2 eq), Et<sub>3</sub>N (2 eq), dry THF, RT, 2 h; (b) PhB(OH)<sub>2</sub> (1.6 equiv), Pd<sub>2</sub>(dba)<sub>3</sub> (0.032 eq), Cy<sub>3</sub>P 20% toluene (0.08 eq), Cs<sub>2</sub>CO<sub>3</sub> (1.7 eq), dioxane, 100 °C, overnight; (c) CF<sub>3</sub>COOH, dry DCM, 0 °C to RT, 2 h; (d) 3-methoxybenzoic acid (1 eq), HATU (1.05 eq), DIPEA (4 eq), dry DMF, RT, 4 h; (e) 1M BBr<sub>3</sub>, dry CH<sub>2</sub>Cl<sub>2</sub>, -78 to 0 °C, then RT, 1 h.

A detailed analysis of <sup>1</sup>H and <sup>13</sup>C-NMR spectra of some (1-benzoylpiperidin-4-yl)(4-chlorophenyl)methanone derivatives revealed the presence of two rotational conformers generated by the rotation of the bond between the variously substituted phenyl ring and the amidic carbonyl group. The splitting of <sup>1</sup>H and <sup>13</sup>C-NMR signals was observed for *ortho*-substituted compounds, since the presence of bulky groups in this position such as Cl (**7c**), Br (**11c**), I (**12c**), CF<sub>3</sub> (**14c**), CH<sub>3</sub> (**13c**), OCH<sub>3</sub> (**15c**), and OCF<sub>3</sub> (**16c**) led to the presence of two rotational conformers. Conversely when the substituents are either absent or are present in *meta* or *para* positions the rotation is free at room temperature and a unique conformer is observed by NMR analysis. In the case of compounds **17c** and

**18c**, the presence of *ortho*-OH (**17c**) or *ortho*-NH<sub>2</sub> (**18c**) groups allows the formation of an intramolecular H-bond between the hydrogen atom of hydroxyl or amino group and the amide C=O oxygen atom, thus inducing a stabilization of only one conformer. Surprisingly, for *ortho*-fluoro derivative **10c** no splitting of signals was observed, despite the non-negligible steric hindrance of the halogen atom. This observation may be explained considering the partial negative charge of both the fluorine atom and the carbonyl oxygen atom, which cause a charge repulsion leading to the stabilization of the conformer where these two atoms maximize their distance. Similarly, the single conformer observed for the *ortho*-nitro derivative **19c** may have the nitro group and the carbonyl oxygen atom distant, due to the repulsion between the partially negatively charged oxygen of the amide C=O and the negatively charged oxygens of the NO<sub>2</sub> group, causing the block of the rotation which leads to the presence of a single conformer. The presence of conformer was verified for a representative compound, (4-(4-chlorobenzoyl)piperidin-1-yl)(2-iodophenyl)methanone **12c**, by acquiring <sup>1</sup>H-NMR spectrum at high temperature (80 °C) in a suitable solvent (DMSO-*d*<sub>6</sub>), in order to overcome the energetic rotational barrier for the different conformers and thus collapse the splitting of signals. As shown in Figures S8-S10, the high temperature increased the interconversion rate between the two rotamers and the spectrum revealed a collapse of the signals of the two conformers, which is particularly evident in the aromatic region of the spectrum.

## CONCLUSIONS

In summary, molecular modeling predictions of the probable binding pose guided chemical modifications of the structure of the initial compound **4** as a first attempt to improve the inhibition potency of this compound on *h*MAGL. The first part of the structural optimization of **4** led to the identification of compound **17b**, which displayed remarkably high MAGL inhibition activity, selectivity for MAGL over FAAH, reversible interaction properties and antiproliferative activity in cancer cells. Therefore, to the best of our knowledge **17b** can now be considered as one of the most active reversible MAGL inhibitors ever reported so far in literature. Finally, the *m*-hydroxyl

substituent of this compound replaces a structural water molecule present in the main crystal structures of *h*MAGL.<sup>18-21</sup> Considering that almost all the known MAGL inhibitors show H-bond interactions only in the proximity of the oxyanion hole, constituted by the backbone NH groups of A51 and M123, the possibility of replacing a water molecule by forming profitable H-bonds also with E53 and H272 residues could provide a new key anchoring point for the development of new MAGL inhibitors. As a further attempt to improve the MAGL inhibition activity of the reported compounds, the replacement of the *p*-chlorophenyl group of compound **17b** with fragments that are characterized by different size and interaction points is currently underway. In the present paper we have modified only the amidic phenyl portion of the scaffold with the insertion of simple and small groups as a first-stage optimization study. It is our purpose now to carry out further modifications of the structure of the best compound **17b**, with the aim of obtaining derivatives that are characterized by an improved MAGL inhibition activity. As a preview of our future optimization work, we have observed that the replacement of the *p*-chlorophenyl ring with a biphenyl ring (compound **6**) leads to about a two-fold increase of activity (compared to compound **7a**). Therefore, as a preliminary attempt to improve the activity of compound **17b**, we synthesized and tested the (4-([1,1'-biphenyl]-4-carbonyl)piperidin-1-yl)(3-hydroxyphenyl)methanone derivative (compound **43**, Scheme 6). As shown in Figure S13, in an agreement with the herein reported data, adding a second phenyl ring in compound **43** led to a two-fold increase of activity with respect to **17b** ( $IC_{50} = 0.46 \pm 0.02 \mu\text{M}$ ), thus confirming the promising possibilities of further improving the inhibition activity of the best derivative of this series of compounds by modifying the *p*-chlorophenyl region of the molecule.

## EXPERIMENTAL SECTION

### Pan Assay Interference Compounds (PAINS) analysis.

The herein reported class of compounds could act as artifacts and promiscuous bioactive molecules. Therefore, a PAINS analysis for the most active compound (**17b**) was carried out in order to analyze and exclude this possibility.



*PAINS substructural features screening.* Baell and Holloway published an interesting paper on the analysis of frequent hitters from screening assays.<sup>24</sup> This report described a number of substructural features which could help to identify compounds that appear as PAINS in many biochemical high throughput screens. In the supplementary information they provided the corresponding filters that have been included in the Filter-it<sup>TM</sup> software. Compound **17b** was thus filtered by using this program and as a result it was recognized as no PAIN molecule because it did not possess any of the substructural features shared by the most common PAINS.

*Interference analysis.* Some PAINS are associated with color that could interfere photometrically with the assay. As reported in the part of MAGL inhibition assay of the Experimental Section, in order to avoid this possibility for each compound concentration a blank analysis was carried out, and the final absorbance values resulted from the subtraction of the absorbance determined by the presence of all the components except the enzyme in the same conditions. Furthermore, a specific analysis for compound **17b** was carried out. The 4-nitrophenylacetate (4-NPA) to 4-nitrophenol (4-NP) conversion curve was prepared at 100  $\mu$ M total concentration of 4-NPA+4-NP in the presence and absence of **17b** at a concentration of 200  $\mu$ M. As shown in the Figure S11, the two resulting curves were superimposable. As a positive control, we analyzed in the same conditions the effects of quercetin at 200  $\mu$ M, that resulted in a shifted curve. Finally, we analyzed the results in the first part of the plot, in the 100-80  $\mu$ M concentration range of 4-NPA (corresponding to 0-20% conversion of 4-NAP to 4-NP). As shown in Figure S11 the two straight lines measured in the presence and absence of **17b** were almost identical, differently from what observed for quercetin, that produced a shifted line, thus suggesting that **17b** did not interfere with the reading at 405 nm in the enzymatic assay.

*Aggregation analysis.* All the enzymatic assays were carried out in the presence of bovine serum albumin (BSA) 0.1 mg/ml. However, in order to further verify the possible formation of aggregates, the MAGL inhibition activity of compound **17b** was also tested in the presence of 0.01% (v/v) Triton X-100 as detergent. With respect to the IC<sub>50</sub> value obtained in the presence of BSA (IC<sub>50</sub> = 0.84  $\pm$

0.04  $\mu\text{M}$ ), a similar result was obtained ( $\text{IC}_{50} = 0.76 \pm 0.02 \mu\text{M}$ ) in the presence of Triton X-100, supporting the notion that the ligand is operating as a monomer rather than an aggregate.<sup>25</sup>

*Thiol reactive analysis.* As reported by Walters and co-workers,<sup>26</sup> promiscuous enzymatic inhibition could be due in some cases to covalent reaction with cysteines on multiple proteins. MAGL inhibition activity of compound **17b** was also tested in the presence of the thiol-containing agent 1,4-dithio-DL-threitol (DTT).<sup>7</sup> As shown in Figure S12, the MAGL- $\text{IC}_{50}$  value of compound **17b** was not influenced by the presence of DTT, as it showed a  $\text{IC}_{50} = 0.80 \pm 0.05 \mu\text{M}$  when assayed with 100  $\mu\text{M}$  DTT, thus excluding the interaction of this compound with the cysteine residues of the MAGL enzyme.

*Selectivity testing and orthogonal assay.* As reported by Dahlin and Walters<sup>27</sup> the selective activity of a compound and the measurement of the activity against the target by using a different readout method are two other steps that contribute to elucidate the PAINS properties. As reported in Table 4 we measured the activity of compound **17b** against FAAH and the results highlighted a MAGL selectivity greater than 119-fold. Furthermore, very recently Saccomanni and co-workers reported the development of an HPLC/UV assay for the evaluation of MAGL inhibitors.<sup>28</sup> Therefore, the activity of compound **17b** against MAGL was also tested by using this method. An aliquot of stock solutions of hMAGL was diluted 1:125 with Tris buffer (pH = 7.2; 10 mM, containing 1.0 mM EDTA) to obtain the working solutions of hMAGL at 1.6 ng/ $\mu\text{l}$ . The stock and working solutions were stored at  $-20 \text{ }^{\circ}\text{C}$ . In a 0.5 ml spin tube containing 75  $\mu\text{l}$  of Tris buffer (pH = 7.2; 10 mM containing 1.0 mM EDTA), 5  $\mu\text{l}$  of working solution hMAGL (8 ng), and 5  $\mu\text{l}$  inhibitor (or solvent as control) were added. Samples were pre-incubated for 30 min at 37  $^{\circ}\text{C}$  and then 5  $\mu\text{l}$  of a solution of 4-NPA in absolute ethanol (4.25 mM) were added. Samples were incubated for 10 min at 37  $^{\circ}\text{C}$ . The enzymatic reaction was stopped by cooling in an ice bath for 10 min and then 20  $\mu\text{l}$  of the reaction mixture were taken and analyzed by HPLC. Thermo Finnigan HPLC system was used to quantify 4-NP formed after enzymatic hydrolysis of 4-NPA by using a UV detector at operation wavelength of 315 nm.

Separation of compounds was carried out on to reverse-phase column (150 mm × 4.6 mm; 5 μm).

The mobile phase, delivered at a flow rate of 1.0 ml/min and consisted of methanol and ammonium acetate buffer (pH 4.0; 10 mM) (53:47, v/v). The sample injection volume was 20 μl. The HPLC system consists of a Thermo Finnigan SpectraSystem SN4000 system controller, coupled with P2000 pump, a SCM1000 degasser and a UV2000 UV detector at operation wavelength of 315 nm. Data were monitored and analyzed using ChromQuest software (Thermo Finnigan, Waltham, MA, USA).

Separation of compounds was carried out at r.t. on to reverse-phase Chrompack HPLC column SS 150 mm × 4.6 mm; 5 μm, with ChromSep guard column intersil 5 ODS-3 (Varian, Palo Alto California).

By using this assay method, compound **17b** showed an IC<sub>50</sub> against MAGL of 1.1 ± 0.3 μM, thus confirming the inhibition activity measured by the colorimetric assay.

### **General Procedures and Materials.**

All solvents and chemicals were used as purchased without further purification. Chromatographic separations were performed on silica gel columns by flash chromatography (Kieselgel 40, 0.040–0.063 mm; Merck). Reactions were followed by thin layer chromatography (TLC) on Merck aluminum silica gel (60 F254) sheets that were visualized under a UV lamp. Evaporation was performed in vacuo (rotating evaporator). Sodium sulfate was always used as the drying agent. Proton (<sup>1</sup>H) and carbon (<sup>13</sup>C) NMR spectra were obtained with a Bruker Avance III 400 MHz spectrometer using the indicated deuterated solvents. Chemical shifts are given in parts per million (ppm) (δ relative to residual solvent peak for <sup>1</sup>H and <sup>13</sup>C). <sup>1</sup>H-NMR spectra are reported in this order: multiplicity and number of protons. Standard abbreviation indicating the multiplicity were used as follows: s = singlet, d = doublet, dd = doublet of doublets, t = triplet, tt = triplet of triplets, dt = doublet of triplets, td = triplet of doublets, q = quartet, m = multiplet, bm = broad multiplet and bs = broad signal. HPLC analysis: all target compounds (i.e., assessed in biological assays) were ≥ 95% pure by HPLC,

confirmed via UV detection ( $\lambda = 254$  nm). Analytical reversed-phase HPLC was conducted using a Kinetex EVO C18 column (5  $\mu$ m, 150  $\times$  4.6 mm, Phenomenex, Inc.); eluent A, water; eluent B, CH<sub>3</sub>CN; after 5 min. at 25% B, a gradient was formed from 25% to 75% of B in 5 min and held at 75% of B for 10 min; flow rate was 1 mL/min. HPLC analyses were performed at 254 nm, with the exception of compound **8** which was analyzed at 226 nm (UV-visible spectrum and superimposition of HPLC chromatograms at 254 e 226 nm of compound **8** are reported in the Supporting Information section). Yields refer to isolated and purified products derived from non-optimized procedures. Compounds **1** and **2** were purchased from Cayman Chemical and **3** was synthesized as previously reported.<sup>16</sup> Compound **4** was characterized as previously reported.<sup>17</sup>

**General procedure for the synthesis of benzoylpiperidines 5, 6, 7a-c, 10a-c, 11a-c, 12a-c, 13a-c, 14a-c, 15b-c, 16a-c, 18c, 19a-c, 20, 30, 31, 44 and benzoylpiperazine 9.** HATU (1.05 equiv) was added to a solution of the appropriate benzoic acid (0.447 mmol, 1 equiv) in dry DMF (2.1 mL), then DIPEA (0.31 mL, 4 equiv) was added dropwise. The resulting mixture was stirred at room temperature for 30 min and then 4-(4-chlorobenzoyl)piperidine **21** (100 mg, 1 equiv) or [1,1'-biphenyl]-4-yl(piperidin-4-yl)methanone **38** (for compounds **6** and **44**), or 1-(4-chlorobenzoyl)piperazine **41** (for compound **9**) was added and left under stirring at room temperature until consumption of starting material (TLC). After this time, DMF was evaporated under reduced pressure and the residue was diluted with water and extracted with EtOAc. The organic layer was washed sequentially with water, saturated brine, dried over Na<sub>2</sub>SO<sub>4</sub> and the solvent was removed under reduced pressure. The residue was purified with a flash column chromatography (silica gel, appropriate mixture of *n*-hexane/ethyl acetate) and pure fractions containing the desired compound were evaporated to dryness affording the amides.

**Synthesis of 4-(4-chlorobenzyl)-1-(4-methoxybenzyl)piperidine (8).** A solution of 4-(4-chlorobenzyl)piperidine **39** (0.812 mmol, 1 eq) in 6.8 mL of DMF was treated with K<sub>2</sub>CO<sub>3</sub> (3 eq) and 4-methoxybenzyl chloride **40** (1.1 eq) and the reaction mixture was stirred at room temperature

overnight. The mixture was diluted with water and extracted into ethyl acetate. The organic extracts were washed successively with water and brine, and the organic solvent was removed under vacuum on a rotary evaporator. Crude product was purified by flash chromatography over silica gel. Elution with *n*-hexane/EtOAc (6:4) afforded the desired compound as a white solid (yield 53%). <sup>1</sup>H-NMR (CDCl<sub>3</sub>) δ (ppm): 1.27-1.37 (m, 2H), 1.41-1.52 (m, 1H), 1.54-1.62 (m, 2H), 1.83-1.94 (m, 2H), 2.49 (d, 2H, *J* = 7.0 Hz), 2.83-2.89 (m, 2H), 3.44 (s, 2H), 3.79 (s, 3H), 6.84 (AA'XX', 2H, *J*<sub>AX</sub> = 8.7 Hz, *J*<sub>AA'XX'</sub> = 2.5 Hz), 7.04 (AA'XX', 2H, *J*<sub>AX</sub> = 8.4 Hz, *J*<sub>AA'XX'</sub> = 2.2 Hz), 7.19-7.24 (m, 4H). <sup>13</sup>C-NMR (CDCl<sub>3</sub>) δ (ppm): 32.18 (2C), 38.01, 42.64, 53.71 (2C), 55.38, 62.87, 113.66 (4C), 128.38, 130.55 (4C), 131.64, 139.33, 158.81. HPLC analysis: retention time = 11.718 min; peak area, 99% (226 nm).

**Procedure for the synthesis of *O*-deprotected benzoylpiperidines 17a-c and 43.** A solution of pure amides **4**, **15b-c** or **44** (0.23 mmol) in anhydrous CH<sub>2</sub>Cl<sub>2</sub> (2.7 mL) was cooled to -78 °C and treated dropwise with a 1.0 M solution of BBr<sub>3</sub> in CH<sub>2</sub>Cl<sub>2</sub> (0.73 mL) under argon. The mixture was left under stirring at the same temperature for 5 min and then at 0 °C for 1 h and finally at RT until starting material was consumed (TLC). The mixture was then diluted with water and extracted with ethyl acetate. The organic phase was washed with brine, dried and concentrated. The crude product was purified by flash chromatography over silica gel. Elution with *n*-hexane/EtOAc (6:4 to 4:6) afforded the desired compounds.

**Procedure of deprotection for the synthesis of compounds 18a-b and 38.** Compounds **30-31** or **37** (0.135 mmol) were dissolved in CH<sub>2</sub>Cl<sub>2</sub> (0.60 mL), cooled to 0 °C, treated with trifluoroacetic acid (0.18 mL) and stirred at rt until consumption of starting material (TLC). The mixture was concentrated to dryness under reduced pressure, diluted with EtOAc and washed with 1M solution NaHCO<sub>3</sub>, then the organic layer was dried over Na<sub>2</sub>SO<sub>4</sub> and concentrated. The crude product was purified by flash chromatography over silica gel. Elution with *n*-hexane/EtOAc (3:7 to 4:6) or CHCl<sub>3</sub>/MeOH 85:15 gave the title compounds.

**Procedure for the synthesis of methyl amino-benzoates 24 and 25.** A solution of the appropriate commercially available aminobenzoic acids **22** or **23** (1.0 g, 1 equiv) in MeOH (20 mL) was cooled

to 0 °C followed by a dropwise addition of thionyl chloride (1.3 mL, 2.5 equiv). The mixture was refluxed for 3 h. After cooling to rt, evaporation of the solvent and neutralization by addition of a saturated aqueous NaHCO<sub>3</sub> solution, the mixture was extracted with EtOAc and the combined organic layers were dried over Na<sub>2</sub>SO<sub>4</sub> and concentrated. Purification by flash chromatography over silica gel and elution with *n*-hexane/EtOAc (7:3) afforded the title compounds.

**Procedure for the synthesis of methyl (*tert*-butoxycarbonyl)amino benzoates **26-27** and *tert*-butyl 4-(4-chlorobenzoyl)piperidine-1-carboxylate **36**.** To a solution of compounds **24-25** or **21** (0.1 g, 1 equiv) in dry THF (1.7 mL) and Et<sub>3</sub>N (2 equiv), (Boc)<sub>2</sub>O (2 equiv for **26** and **27**, 1.2 equiv for **36**) was added and the reaction was stirred at room temperature until disappearance of starting material (TLC). The solvent was evaporated in vacuo and the residue was dissolved in EtOAc, washed with 1M NaHCO<sub>3</sub>, water and brine. Then the organic layer was dried over Na<sub>2</sub>SO<sub>4</sub> and concentrated. The crude product was purified by flash chromatography over silica gel. Elution with *n*-hexane/EtOAc (95:5 to 8:2) afforded the desired compounds.

**Procedure for the synthesis of (*tert*-butoxycarbonyl)amino benzoic acids **28-29** and [1,1'-biphenyl]-4-carboxylic acid **35**.** Methyl esters **26-27** or **34** (0.1 g) were dissolved in a 1:1 v/v mixture of THF/methanol (4 mL) and treated with 1.2 mL of 2N aqueous solution of LiOH. The reaction was stirred overnight, then the solvents were evaporated, and the residue was treated with 1 N aqueous HCl and extracted with EtOAc. The organic phase was dried and evaporated to afford the pure desired carboxylic acid derivatives.

**Procedure for the synthesis of methyl 4-bromobenzoate (**33**).** 4-Bromobenzoic acid **32** (250 mg) was dissolved in MeOH until complete dissolution (20 mL), then conc. H<sub>2</sub>SO<sub>4</sub> (cat.) was added dropwise and the mixture was refluxed overnight. After being cooled to rt, the solvent was evaporated in vacuo and the residue was dissolved in EtOAc, washed with 1M NaHCO<sub>3</sub>, then the organic layer was dried over Na<sub>2</sub>SO<sub>4</sub> and concentrated. Pure **33** was obtained as a crystalline light-yellow solid (1.13 mmol, 92% yield) and it was used in the next step without any further purification.

**Procedure for the synthesis of methyl [1,1'-biphenyl]-4-carboxylate (34).** A solution of Pd(OAc)<sub>2</sub> (0.03 equiv) and triphenylphosphine (0.15 equiv) in toluene (9.0 mL) was stirred at rt under argon for 10 min. After that period, the bromo-aryl precursor **33** (0.93 mmol, 1 equiv), K<sub>2</sub>CO<sub>3</sub> (1.5 equiv), and phenylboronic acid (2 equiv) were sequentially added. The resulting mixture was heated at 100 °C in a sealed vial under argon overnight. After being cooled to rt, the mixture was diluted with water and extracted with EtOAc. The combined organic phase was dried and concentrated. The crude product was purified by flash chromatography over silica gel. Elution with *n*-hexane with 1% EtOAc afforded **34** as a white solid (0.779 mmol, 84% yield).

**Procedure for the synthesis of *tert*-butyl 4-([1,1'-biphenyl]-4-carbonyl)piperidine-1-carboxylate (37).** A solution of **36** (0.182 g, 0.562 mmol, 1 equiv) in anhydrous dioxane (1.7 mL) was sequentially treated, under nitrogen, with cesium carbonate (1.7 equiv), phenylboronic acid (1.6 equiv), Pd<sub>2</sub>(dba)<sub>3</sub> (0.032 equiv), and a 20% solution of tricyclohexylphosphine in toluene (0.08 equiv). The reaction was heated at 100 °C in a sealed vial under argon overnight. The reaction mixture was then cooled to rt, diluted with EtOAc, and filtered through a Celite pad. The organic filtrate was concentrated under vacuum, and the crude product was purified by flash chromatography (*n*-hexane/EtOAc 9:1) to yield pure **37** (0.535 mmol, 95% yield).

**(1-([1,1'-Biphenyl]-4-carbonyl)piperidin-4-yl)(4-chlorophenyl)methanone (5).** Yellow solid; yield 67% from **21** and **35**; <sup>1</sup>H-NMR (CDCl<sub>3</sub>) δ (ppm): 1.78-2.07 (m, 4H), 3.00-3.26 (bm, 2H), 3.47-3.56 (m, 1H), 3.87-4.07 (bm, 1H), 4.60-4.80 (bm, 1H), 7.38 (tt, 1H, *J* = 7.3, 1.6 Hz), 7.43-7.52 (m, 6H), 7.57-7.62 (m, 2H), 7.63 (AA'XX', 2H, *J*<sub>AX</sub> = 8.5 Hz, *J*<sub>AA'/XX'</sub> = 1.9 Hz), 7.90 (AA'XX', 2H, *J*<sub>AX</sub> = 8.8 Hz, *J*<sub>AA'/XX'</sub> = 2.2 Hz). <sup>13</sup>C-NMR (CDCl<sub>3</sub>) δ (ppm): 28.73 (2C), 43.46, 127.27 (2C), 127.34 (2C), 127.61 (2C), 127.91, 129.01 (2C), 129.29 (2C), 129.83 (2C), 134.08, 134.78, 139.90, 140.35, 142.76, 170.45, 200.53. HPLC analysis: retention time = 13.758 min; peak area, 99% (254 nm).

**(4-([1,1'-Biphenyl]-4-carbonyl)piperidin-1-yl)(4-chlorophenyl)methanone (6).** Light-yellow solid; yield 84% from **38** and 4-chlorobenzoic acid; <sup>1</sup>H-NMR (CDCl<sub>3</sub>) δ (ppm): 1.76-2.15 (m, 4H), 3.00-3.28 (bm, 2H), 3.54-3.63 (m, 1H), 3.76-3.95 (bm, 1H), 4.58-4.78 (bm, 1H), 7.36-7.44 (m, 5H),

7.45-7.51 (m, 2H), 7.61-7.65 (m, 2H), 7.71 (AA'XX', 2H,  $J_{AX} = 8.6$  Hz,  $J_{AA'/XX'} = 1.9$  Hz), 8.03 (AA'XX', 2H,  $J_{AX} = 8.6$  Hz,  $J_{AA'/XX'} = 1.9$  Hz).  $^{13}\text{C-NMR}$  ( $\text{CDCl}_3$ )  $\delta$  (ppm): 28.75 (2C), 43.44, 127.37 (3C), 127.59 (2C), 128.48, 128.57 (2C), 128.92 (2C), 129.00 (2C), 129.12, 134.35, 134.42, 135.87, 139.79, 146.18, 169.52, 201.21. HPLC analysis: retention time = 13.747 min; peak area, 97% (254 nm).

**Piperidine-1,4-diylbis((4-chlorophenyl)methanone) (7a).** White solid; yield 60% from **21** and 4-chlorobenzoic acid;  $^1\text{H-NMR}$  ( $\text{CDCl}_3$ )  $\delta$  (ppm): 1.72-2.05 (m, 4H), 3.00-3.20 (bm, 2H), 3.45-3.54 (m, 1H), 3.72-3.96 (bm, 1H), 4.53-4.72 (bm, 1H), 7.34-7.41 (m, 4H), 7.46 (AA'XX', 2H,  $J_{AX} = 8.8$  Hz,  $J_{AA'/XX'} = 2.2$  Hz), 7.89 (AA'XX', 2H,  $J_{AX} = 8.7$  Hz,  $J_{AA'/XX'} = 2.2$  Hz).  $^{13}\text{C-NMR}$  ( $\text{CDCl}_3$ )  $\delta$  (ppm): 28.65 (2C), 43.31, 128.57 (2C), 128.93 (2C), 129.31 (2C), 129.80 (2C), 134.03, 134.37, 135.93, 139.96, 169.52, 200.40. HPLC analysis: retention time = 13.001 min; peak area, 98% (254 nm).

**(4-(4-Chlorobenzoyl)piperidin-1-yl)(3-chlorophenyl)methanone (7b).** Light-yellow solid; yield 68% from **21** and 3-chlorobenzoic acid;  $^1\text{H-NMR}$  ( $\text{CDCl}_3$ )  $\delta$  (ppm): 1.73-2.09 (m, 4H), 2.98-3.23 (bm, 2H), 3.45-3.55 (m, 1H), 3.74-3.91 (bm, 1H), 4.57-4.73 (bm, 1H), 7.29 (dt, 1H,  $J = 7.4, 1.5$  Hz), 7.35 (t, 1H,  $J = 8.0$  Hz), 7.38-7.41 (m, 2H), 7.46 (AA'XX', 2H,  $J_{AX} = 8.8$  Hz,  $J_{AA'/XX'} = 2.2$  Hz), 7.89 (AA'XX', 2H,  $J_{AX} = 8.8$  Hz,  $J_{AA'/XX'} = 2.2$  Hz).  $^{13}\text{C-NMR}$  ( $\text{CDCl}_3$ )  $\delta$  (ppm): 28.60 (2C), 43.24, 125.03, 127.15, 129.27 (2C), 129.78 (2C), 129.93, 130.03, 133.97, 134.71, 137.72, 139.91, 168.93, 200.35. HPLC analysis: retention time = 12.961 min; peak area, 99% (254 nm).

**(4-(4-Chlorobenzoyl)piperidin-1-yl)(2-chlorophenyl)methanone (7c).** Light-yellow solid; yield 58% from **21** and 2-chlorobenzoic acid;  $^1\text{H-NMR}$  ( $\text{CDCl}_3$ )  $\delta$  (ppm): 1.65-2.04 (m, 4H), 3.02-3.28 (m, 2H), 3.40-3.60 (m, 2H), 4.75 (tt, 1H,  $J = 10.9, 4.0$  Hz), 7.30-7.35 (m, 3H), 7.37-7.43 (m, 1H), 7.43-7.48 (m, 2H), 7.86-7.90 (m, 2H).  $^{13}\text{C-NMR}$  ( $\text{CDCl}_3$ ; asterisk denotes isomer peaks)  $\delta$  (ppm): 28.41, 28.59, 28.66\*, 41.01, 41.16\*, 43.18, 43.38\*, 45.87, 46.57\*, 127.21\*, 127.41, 127.67\*, 127.84, 129.24\*, 129.27, 129.69\*, 129.78 (4C), 129.86\*, 130.21\*, 130.32, 130.37, 130.53\*, 134.01, 134.06\*, 135.97\*, 136.08, 139.80\*, 139.90, 166.90\*, 167.04, 200.33\*, 200.45. HPLC analysis: retention time = 12.699 min; peak area, 99% (254 nm).



**(4-(4-Chlorobenzoyl)piperazin-1-yl)(4-methoxyphenyl)methanone (9).** White solid; yield 61% from **41** and 4-methoxybenzoic acid **42**;  $^1\text{H-NMR}$  ( $\text{CDCl}_3$ )  $\delta$  (ppm): 3.43-3.78 (bm, 8H), 3.84 (s, 3H), 6.90-6.95 (m, 2H), 7.34-7.44 (bm, 6H).  $^{13}\text{C-NMR}$  ( $\text{CDCl}_3$ )  $\delta$  (ppm): 55.52, 114.04 (2C), 126.99, 128.78 (2C), 129.08 (2C), 129.39 (2C), 133.55, 136.42, 161.31, 169.75, 170.87. HPLC analysis: retention time = 10.629 min; peak area, 97% (254 nm).

**(4-(4-Chlorobenzoyl)piperidin-1-yl)(4-fluorophenyl)methanone (10a).** Light-yellow solid; yield 62% from **21** and 4-fluorobenzoic acid;  $^1\text{H-NMR}$  ( $\text{CDCl}_3$ )  $\delta$  (ppm): 1.72-2.05 (m, 4H), 3.00-3.20 (bm, 2H), 3.45-3.55 (m, 1H), 3.72-4.00 (bm, 1H), 4.50-4.70 (bm, 1H), 7.10 (double AA'XX', 2H,  $^3J_{\text{HF-o}} = 9.5$  Hz,  $J_{\text{AX}} = 8.7$  Hz,  $J_{\text{AA'}/\text{XX}'} = 2.4$  Hz), 7.40-7.49 (m, 4H), 7.89 (AA'XX', 2H,  $J_{\text{AX}} = 8.7$  Hz,  $J_{\text{AA'}/\text{XX}'} = 2.2$  Hz).  $^{13}\text{C-NMR}$  ( $\text{CDCl}_3$ )  $\delta$  (ppm): 28.63 (2C), 43.32, 115.69 (d, 2C,  $J = 22.1$  Hz), 129.26 (2C), 129.30 (d, 2C,  $J = 9.1$  Hz), 129.78 (2C), 132.00 (d,  $J = 3.0$  Hz), 134.00, 139.90, 163.49 (d,  $J = 249.5$  Hz), 169.65, 200.41. HPLC analysis: retention time = 12.464 min; peak area, 97% (254 nm).

**(4-(4-Chlorobenzoyl)piperidin-1-yl)(3-fluorophenyl)methanone (10b).** Light-yellow solid; yield 55% from **21** and 3-fluorobenzoic acid;  $^1\text{H-NMR}$  ( $\text{CDCl}_3$ )  $\delta$  (ppm): 1.73-2.08 (m, 4H), 3.00-3.22 (bm, 2H), 3.46-3.54 (m, 1H), 3.75-3.92 (bm, 1H), 4.58-4.74 (bm, 1H), 7.09-7.14 (m, 2H), 7.15 (dt, 1H,  $J = 7.8, 1.2$  Hz), 7.36-7.42 (m, 1H), 7.46 (AA'XX', 2H,  $J_{\text{AX}} = 8.8$  Hz,  $J_{\text{AA'}/\text{XX}'} = 2.2$  Hz), 7.89 (AA'XX', 2H,  $J_{\text{AX}} = 8.8$  Hz,  $J_{\text{AA'}/\text{XX}'} = 2.2$  Hz).  $^{13}\text{C-NMR}$  ( $\text{CDCl}_3$ )  $\delta$  (ppm): 28.61 (2C), 43.26, 114.27 (d,  $J = 22.1$  Hz), 116.83, (d,  $J = 21.1$  Hz), 122.60 (d,  $J = 3.0$  Hz), 129.27 (2C), 129.79 (2C), 130.46 (d,  $J = 8.0$  Hz), 133.99, 138.06 (d,  $J = 7.0$  Hz), 139.91, 162.65 (d,  $J = 248.5$  Hz), 169.04, 200.37. HPLC analysis: retention time = 12.519 min; peak area, 99% (254 nm).

**(4-(4-Chlorobenzoyl)piperidin-1-yl)(2-fluorophenyl)methanone (10c).** Light-yellow solid; yield 64% from **21** and 2-fluorobenzoic acid;  $^1\text{H-NMR}$  ( $\text{CDCl}_3$ )  $\delta$  (ppm): 1.73-1.87 (m, 3H), 1.98-2.06 (m, 1H), 3.02-3.29 (m, 2H), 3.42-3.53 (m, 1H), 3.63-3.72 (m, 1H), 4.68-4.76 (m, 1H), 7.09 (t, 1H,  $J = 9.6$  Hz), 7.21 (td, 1H,  $J = 8.0, 0.9$  Hz), 7.36-7.42 (m, 2H), 7.46 (AA'XX', 2H,  $J_{\text{AX}} = 8.6$  Hz,  $J_{\text{AA'}/\text{XX}'} = 2.1$  Hz), 7.89 (AA'XX', 2H,  $J_{\text{AX}} = 8.7$  Hz,  $J_{\text{AA'}/\text{XX}'} = 2.1$  Hz).  $^{13}\text{C-NMR}$  ( $\text{CDCl}_3$ )  $\delta$  (ppm): 28.55, 28.60, 41.43, 43.32, 46.54, 115.89 (d,  $J = 21.1$  Hz), 124.32 (d,  $J = 18.1$  Hz), 124.83 (d,  $J = 3.0$  Hz), 129.14

(d,  $J = 4.0$  Hz), 129.27 (2C), 129.80 (2C), 131.38 (d,  $J = 8.0$  Hz), 134.07, 139.86, 158.26 (d,  $J = 248.5$  Hz), 165.34, 200.42. HPLC analysis: retention time = 12.439 min; peak area, 98% (254 nm).

**(1-(4-Bromobenzoyl)piperidin-4-yl)(4-chlorophenyl)methanone (11a).** Yellow solid; yield 65% from **21** and 4-bromobenzoic acid;  $^1\text{H-NMR}$  ( $\text{CDCl}_3$ )  $\delta$  (ppm): 1.64-2.00 (m, 4H), 3.04-3.28 (bm, 2H), 3.46-3.53 (m, 1H), 3.80-3.90 (bm, 1H), 4.58-4.70 (bm, 1H), 7.30 (AA'XX', 2H,  $J_{AX} = 8.4$  Hz,  $J_{AA'/XX'} = 2.1$  Hz), 7.46 (AA'XX', 2H,  $J_{AX} = 8.6$  Hz,  $J_{AA'/XX'} = 2.2$  Hz), 7.55 (AA'XX', 2H,  $J_{AX} = 8.4$  Hz,  $J_{AA'/XX'} = 2.1$  Hz), 7.89 (AA'XX', 2H,  $J_{AX} = 8.6$  Hz,  $J_{AA'/XX'} = 2.1$  Hz).  $^{13}\text{C-NMR}$  ( $\text{CDCl}_3$ )  $\delta$  (ppm): 28.66 (2C), 43.33, 124.18, 128.78 (2C), 129.33 (2C), 129.83 (2C), 131.92 (2C), 134.02, 134.84, 140.00, 169.58, 200.42. HPLC analysis: retention time = 13.127 min; peak area, 98% (254 nm).

**(1-(3-Bromobenzoyl)piperidin-4-yl)(4-chlorophenyl)methanone (11b).** Yellow solid; yield 30% from **21** and 3-bromobenzoic acid;  $^1\text{H-NMR}$  ( $\text{CDCl}_3$ )  $\delta$  (ppm): 1.74-2.03 (m, 4H), 3.05-3.20 (bm, 2H), 3.47-3.54 (m, 1H), 3.78-3.90 (bm, 1H), 4.64-4.67 (bm, 1H), 7.27-7.35 (m, 2H), 7.47 (AA'XX', 2H,  $J_{AX} = 8.6$  Hz,  $J_{AA'/XX'} = 2.0$  Hz), 7.55-7.57 (m, 2H), 7.89 (AA'XX', 2H,  $J_{AX} = 8.7$  Hz,  $J_{AA'/XX'} = 2.1$  Hz).  $^{13}\text{C-NMR}$  ( $\text{CDCl}_3$ )  $\delta$  (ppm): 28.66 (2C), 43.31, 122.83, 125.54, 129.34 (2C), 129.84 (2C), 130.06, 130.32, 132.93, 134.02, 137.99, 140.00, 168.86, 200.41. HPLC analysis: retention time = 13.126 min; peak area, 97% (254 nm).

**(1-(2-Bromobenzoyl)piperidin-4-yl)(4-chlorophenyl)methanone (11c).** Orange solid; yield 57% from **21** and 2-bromobenzoic acid;  $^1\text{H-NMR}$  ( $\text{CDCl}_3$ ; asterisk denotes isomer peaks)  $\delta$  (ppm): 1.65-2.07 (m, 4H), 3.04-3.15 (m, 1H), 3.20-3.28 (m, 1H), 3.42-3.59 (m, 2H), 4.69-4.80 (m, 1H), 7.22-7.31 (m, 2H), 7.34 (dd, 1H,  $J = 7.0, 1.1$  Hz), 7.38\* (dd, 1H,  $J = 8.3, 1.1$  Hz), 7.44-7.48 (m, 2H), 7.56-7.61 (m, 1H), 7.86-7.90 (m, 2H).  $^{13}\text{C-NMR}$  ( $\text{CDCl}_3$ ; asterisk denotes isomer peaks)  $\delta$  (ppm): 28.36\*, 28.39, 28.60, 28.65\*, 41.01, 41.18\*, 43.21, 43.43\*, 45.96\*, 46.63, 119.21, 119.36\*, 127.59\*, 127.75, 127.83, 127.97\*, 129.28\*, 129.31 (2C), 129.81 (2C), 130.34\*, 130.45, 132.86\*, 133.09, 134.04, 134.09\*, 138.18\*, 138.31, 139.86, 139.95\*, 167.74\*, 167.89, 200.36\*, 200.48. HPLC analysis: retention time = 12.798 min; peak area, 97% (254 nm).

**(4-(4-Chlorobenzoyl)piperidin-1-yl)(4-iodophenyl)methanone (12a).** Off-white solid; yield 72% from **21** and 4-iodobenzoic acid;  $^1\text{H-NMR}$  ( $\text{CDCl}_3$ )  $\delta$  (ppm): 1.71-2.08 (m, 4H), 2.98-3.20 (bm, 2H), 3.44-3.53 (m, 1H), 3.74-3.92 (bm, 1H), 4.57-4.72 (bm, 1H), 7.16 (AA'XX', 2H,  $J_{AX} = 8.4$  Hz,  $J_{AA'/XX'} = 2.0$  Hz), 7.46 (AA'XX', 2H,  $J_{AX} = 8.7$  Hz,  $J_{AA'/XX'} = 2.2$  Hz), 7.76 (AA'XX', 2H,  $J_{AX} = 8.4$  Hz,  $J_{AA'/XX'} = 2.0$  Hz), 7.89 (AA'XX', 2H,  $J_{AX} = 8.7$  Hz,  $J_{AA'/XX'} = 2.2$  Hz).  $^{13}\text{C-NMR}$  ( $\text{CDCl}_3$ )  $\delta$  (ppm): 28.61 (2C), 43.26, 95.97, 128.74 (2C), 129.27 (2C), 129.78 (2C), 133.99, 135.39, 137.79 (2C), 139.91, 169.60, 200.36. HPLC analysis: retention time = 13.341 min; peak area, 99% (254 nm).

**(4-(4-Chlorobenzoyl)piperidin-1-yl)(3-iodophenyl)methanone (12b).** Light-yellow solid; yield 51% from **21** and 3-iodobenzoic acid;  $^1\text{H-NMR}$  ( $\text{CDCl}_3$ )  $\delta$  (ppm): 1.73-2.08 (m, 4H), 3.00-3.23 (bm, 2H), 3.46-3.55 (m, 1H), 3.75-3.90 (bm, 1H), 4.57-4.73 (bm, 1H), 7.15 (dd, 1H,  $J = 8.4, 7.6$  Hz), 7.37 (dt, 1H,  $J = 7.9, 1.3$  Hz), 7.47 (AA'XX', 2H,  $J_{AX} = 8.8$  Hz,  $J_{AA'/XX'} = 2.2$  Hz), 7.74-7.78 (m, 2H), 7.89 (AA'XX', 2H,  $J_{AX} = 8.8$  Hz,  $J_{AA'/XX'} = 2.2$  Hz).  $^{13}\text{C-NMR}$  ( $\text{CDCl}_3$ )  $\delta$  (ppm): 28.62 (2C), 43.27, 94.38, 126.05, 129.30 (2C), 129.81 (2C), 130.34, 134.01, 135.79, 138.05, 138.79, 139.94, 168.66, 200.37. HPLC analysis: retention time = 13.301 min; peak area, 98% (254 nm).

**(4-(4-Chlorobenzoyl)piperidin-1-yl)(2-iodophenyl)methanone (12c).** Yellow solid; yield 57% from **21** and 2-iodobenzoic acid;  $^1\text{H-NMR}$  ( $\text{CDCl}_3$ ; asterisk denotes isomer peaks)  $\delta$  (ppm): 1.65-2.15 (m, 4H), 3.05-3.15 (m, 1H), 3.20-3.30 (m, 1H), 3.45-3.60 (m, 2H), 4.68-4.80 (m, 1H), 7.05-7.11 (m, 1H), 7.18\* (dd, 1H,  $J = 7.6, 1.6$  Hz), 7.24 (dd, 1H,  $J = 7.6, 1.6$  Hz), 7.36-7.43 (m, 1H), 7.44-7.48 (m, 2H), 7.81-7.86 (m, 1H), 7.86-7.91 (m, 2H).  $^1\text{H-NMR}$  ( $\text{DMSO-}d_6$ ; asterisk denotes isomer peaks)  $\delta$  (ppm): 1.38-1.65 (m, 2H), 1.67-1.80 (m, 1H), 1.85-1.96 (m, 1H), 2.93-3.05 (m, 1H), 3.09-3.30 (m, 2H), 3.70-3.82 (m, 1H), 4.47-4.60 (m, 1H), 7.12-7.19 (m, 1H), 7.24\* (dd, 1H,  $J = 7.4, 1.2$  Hz), 7.29 (dd, 1H,  $J = 7.5, 1.3$  Hz), 7.43-7.49 (m, 1H), 7.58-7.64 (m, 2H), 7.85-7.90 (m, 1H), 7.90-8.05 (m, 2H).  $^1\text{H-NMR}$  ( $\text{DMSO-}d_6$ ; 80 °C)  $\delta$  (ppm): 1.50-1.80 (bm, 3H), 1.88-1.99 (bm, 1H), 3.00-3.35 (bm, 3H), 3.68-3.77 (m, 1H), 4.44-4.55 (bm, 1H), 7.15 (td, 1H,  $J = 7.7, 1.7$  Hz), 7.23-7.27 (bm, 1H), 7.46 (td, 1H,  $J = 7.5, 1.1$  Hz), 7.58 (AA'XX', 2H,  $J_{AX} = 8.8$  Hz,  $J_{AA'/XX'} = 2.3$  Hz), 7.88 (dd, 1H,  $J = 7.9, 0.8$  Hz), 8.00 (AA'XX', 2H,  $J_{AX} = 8.7$  Hz,  $J_{AA'/XX'} = 2.2$  Hz).  $^{13}\text{C-NMR}$  ( $\text{CDCl}_3$ ; asterisk denotes

isomer peaks)  $\delta$  (ppm): 28.26\*, 28.37, 28.61, 28.66\*, 41.06, 41.20\*, 43.24, 43.45\*, 46.13, 46.71\*, 92.44, 92.70\*, 126.87\*, 127.20, 128.42\*, 128.68, 129.30\*, 129.33, 129.83 (3C), 130.31\*, 130.39, 134.03, 134.08\*, 139.25, 139.57\*, 139.90\*, 139.98, 142.43, 142.56\*, 169.42\*, 169.52, 200.38\*, 200.49.  $^{13}\text{C}$ -NMR (DMSO- $d_6$ ; asterisk denotes isomer peaks)  $\delta$  (ppm): 27.77, 27.94\*, 28.07\*, 28.36, 40.20, 42.24\*, 42.38, 45.40\*, 45.94, 92.90, 93.17\*, 126.79, 126.98\*, 128.29, 128.47\*, 128.92 (4C), 130.17, 130.21\*, 134.01, 138.15, 138.58\*, 138.88, 142.30, 142.41\*, 167.98, 168.09\*, 200.77\*, 200.79.  $^{13}\text{C}$ -NMR (DMSO- $d_6$ ; 80 °C)  $\delta$  (ppm): 27.36, 27.83, 42.05, 45.30, 92.00, 126.58, 127.94, 128.46 (2C), 129.64 (2C), 129.73, 134.05, 137.73, 138.45, 142.17, 167.75, 200.42. HPLC analysis: retention time = 12.972 min; peak area, 99% (254 nm).

**(4-(4-Chlorobenzoyl)piperidin-1-yl)(*p*-tolyl)methanone (13a).** Yellow solid; yield 50% from **21** and *p*-toluic acid;  $^1\text{H}$ -NMR ( $\text{CDCl}_3$ )  $\delta$  (ppm): 1.74-2.00 (m, 4H), 2.38 (s, 3H), 2.95-3.16 (bm, 2H), 3.44-3.55 (m, 1H), 3.80-4.15 (bm, 1H), 4.45-4.53 (bm, 1H), 7.19-7.22 (m, 2H), 7.29-7.33 (m, 2H), 7.46 (AA'XX', 2H,  $J_{AX} = 8.6$  Hz,  $J_{AA'/XX'} = 2.1$  Hz), 7.89 (AA'XX', 2H,  $J_{AX} = 8.6$  Hz,  $J_{AA'/XX'} = 2.1$  Hz).  $^{13}\text{C}$ -NMR ( $\text{CDCl}_3$ )  $\delta$  (ppm): 21.49, 28.71 (2C), 43.49, 127.13 (2C), 129.21 (2C), 129.26 (2C), 129.82 (2C), 133.05, 134.10, 139.85, 139.96, 170.80, 200.56. HPLC analysis: retention time = 12.754 min; peak area, 97% (254 nm).

**(4-(4-Chlorobenzoyl)piperidin-1-yl)(*m*-tolyl)methanone (13b).** Orange solid; yield 51% from **21** and *m*-toluic acid;  $^1\text{H}$ -NMR ( $\text{CDCl}_3$ )  $\delta$  (ppm): 1.74-2.00 (m, 4H), 2.37 (s, 3H), 3.00-3.18 (bm, 2H), 3.45-3.53 (m, 1H), 3.80-4.00 (bm, 1H), 4.55-4.80 (bm, 1H), 7.77-7.24 (m, 3H), 7.28 (t, 1H,  $J = 7.8$  Hz), 7.46 (AA'XX', 2H,  $J_{AX} = 8.7$  Hz,  $J_{AA'/XX'} = 2.2$  Hz), 7.89 (AA'XX', 2H,  $J_{AX} = 8.7$  Hz,  $J_{AA'/XX'} = 2.2$  Hz).  $^{13}\text{C}$ -NMR ( $\text{CDCl}_3$ )  $\delta$  (ppm): 21.47, 28.70 (2C), 43.47, 123.85, 127.55, 128.43 (2C), 129.26 (2C), 129.80, 130.48, 134.08, 136.02, 138.53, 139.86, 170.77, 200.54. HPLC analysis: retention time = 12.766 min; peak area, 96% (254 nm).

**(4-(4-Chlorobenzoyl)piperidin-1-yl)(*o*-tolyl)methanone (13c).** Orange solid; yield 46% from **21** and *o*-toluic acid;  $^1\text{H}$ -NMR ( $\text{CDCl}_3$ ; asterisk denotes isomer peaks)  $\delta$  (ppm): 1.68-1.85 (m, 3H), 1.98-2.08 (m, 1H), 2.30\* (s, 3H), 2.34 (s, 3H), 2.97-3.16 (m, 2H), 3.42-3.55 (m, 1H), 3.56-3.65 (m, 1H),

4.70-4.83 (m, 1H), 7.11-7.30 (m, 4H), 7.46 (AA'XX', 2H,  $J_{AX} = 8.8$  Hz,  $J_{AA'/XX'} = 2.2$  Hz), 7.88 (AA'XX', 2H,  $J_{AX} = 8.8$  Hz,  $J_{AA'/XX'} = 2.0$  Hz).  $^{13}\text{C}$ -NMR ( $\text{CDCl}_3$ ; asterisk denotes isomer peaks)  $\delta$  (ppm): 19.10, 19.21\*, 28.55\*, 28.81, 28.95\*, 40.98, 43.30\*, 43.53, 46.11\*, 46.48, 125.81, 125.96\*, 126.16, 128.99, 129.29 (2C), 129.79 (2C), 130.49, 130.66\*, 134.05, 134.10, 134.41\*, 136.32, 139.92, 170.07\*, 179.17, 200.46, 200.56\*. HPLC analysis: retention time = 12.588 min; peak area, 97% (254 nm).

**(4-(4-Chlorobenzoyl)piperidin-1-yl)(4-(trifluoromethyl)phenyl)methanone (14a)**. Orange solid; yield 54% from **21** and 4-(trifluoromethyl)benzoic acid;  $^1\text{H}$ -NMR ( $\text{CDCl}_3$ )  $\delta$  (ppm): 1.73-2.10 (m, 4H), 3.02-3.24 (bm, 2H), 3.48-3.56 (m, 1H), 3.71-3.83 (bm, 1H), 4.61-4.75 (bm, 1H), 7.47 (AA'XX', 2H,  $J_{AX} = 8.8$  Hz,  $J_{AA'/XX'} = 2.2$  Hz), 7.51-7.55 (m, 2H), 7.67-7.71 (m, 2H), 7.89 (AA'XX', 2H,  $J_{AX} = 8.7$  Hz,  $J_{AA'/XX'} = 2.2$  Hz).  $^{13}\text{C}$ -NMR ( $\text{CDCl}_3$ )  $\delta$  (ppm): 28.64 (2C), 43.22, 123.84 (q,  $J = 272.7$  Hz), 125.79 (q, 2C,  $J = 4.0$  Hz), 127.37, 129.33 (2C), 129.82 (2C), 131.81 (q,  $J = 32.2$  Hz), 133.99, 139.63 (q, 2C,  $J = 1.0$  Hz), 140.02, 169.08, 200.33. HPLC analysis: retention time = 13.273 min; peak area, 96% (254 nm).

**(4-(4-Chlorobenzoyl)piperidin-1-yl)(3-(trifluoromethyl)phenyl)methanone (14b)**. Orange solid; yield 41% from **21** and 3-(trifluoromethyl)benzoic acid;  $^1\text{H}$ -NMR ( $\text{CDCl}_3$ )  $\delta$  (ppm): 1.74-2.09 (m, 4H), 3.02-3.28 (bm, 2H), 3.46-3.57 (m, 1H), 3.70-3.88 (bm, 1H), 4.58-4.76 (bm, 1H), 7.47 (AA'XX', 2H,  $J_{AX} = 8.7$  Hz,  $J_{AA'/XX'} = 2.2$  Hz), 7.55 (t, 1H,  $J = 8.3$  Hz), 7.59-7.63 (m, 1H), 7.67-7.71 (m, 2H), 7.89 (AA'XX', 2H,  $J_{AX} = 8.7$  Hz,  $J_{AA'/XX'} = 2.2$  Hz).  $^{13}\text{C}$ -NMR ( $\text{CDCl}_3$ )  $\delta$  (ppm): 28.59 (2C), 43.19, 123.77 (q,  $J = 273.7$  Hz), 124.04, 126.59, 129.29 (3C), 129.80 (2C), 130.30, 131.24 (q,  $J = 33.2$  Hz), 133.98, 136.82, 139.97, 168.95, 200.31. HPLC analysis: retention time = 13.234 min; peak area, 98% (254 nm).

**(4-(4-Chlorobenzoyl)piperidin-1-yl)(2-(trifluoromethyl)phenyl)methanone (14c)**. Orange solid; yield 55% from **21** and 2-(trifluoromethyl)benzoic acid;  $^1\text{H}$ -NMR ( $\text{CDCl}_3$ ; asterisk denotes isomer peaks)  $\delta$  (ppm): 1.65-1.84 (m, 2H), 1.97-2.08 (m, 2H), 3.03-3.18 (m, 2H), 3.40-3.53 (m, 2H), 4.68-4.77 (m, 1H), 7.32\* (d, 1H,  $J = 7.8$  Hz), 7.37 (d, 1H,  $J = 7.6$  Hz), 7.43-7.48 (m, 2H), 7.49-7.55 (m,

1H), 7.57-7.63 (m, 1H), 7.69-7.73 (m, 1H), 7.85-7.90 (m, 2H). <sup>13</sup>C-NMR (CDCl<sub>3</sub>; asterisk denotes isomer peaks) δ (ppm): 27.77\*, 28.16, 28.23\*, 28.62, 41.10, 41.16\*, 43.17, 43.20\*, 46.60, 46.63\*, 123.77\* (q, *J* = 274.2 Hz), 123.80 (q, *J* = 273.7 Hz), 126.71 (q, *J* = 4.7 Hz), 126.73 (q, *J* = 31.9 Hz), 126.94\* (q, *J* = 5.0 Hz), 127.22\*, 127.25, 128.56, 128.93\*, 129.26 (2C), 129.31\* (2C), 129.79\* (2C), 129.81 (2C), 132.20\*, 132.44, 133.98, 134.05\*, 135.01\* (q, *J* = 2.0 Hz), 135.10 (q, *J* = 2.0 Hz), 139.83\*, 139.98, 167.41\*, 167.56, 200.20\*, 200.48. HPLC analysis: retention time = 13.008 min; peak area, 96% (254 nm).

**(4-(4-Chlorobenzoyl)piperidin-1-yl)(3-methoxyphenyl)methanone (15b).** White solid; yield 67% from **21** and 3-methoxybenzoic acid; <sup>1</sup>H-NMR (CDCl<sub>3</sub>) δ (ppm): 1.72-2.02 (m, 4H), 3.00-3.20 (bm, 2H), 3.45-3.53 (m, 1H), 3.82 (s, 3H), 3.80-3.95 (bm, 1H), 4.60-4.75 (bm, 1H), 6.93-6.98 (m, 3H), 7.28-7.33 (m, 1H), 7.46 (AA'XX', 2H, *J*<sub>AX</sub> = 8.8 Hz, *J*<sub>AA'/XX'</sub> = 2.2 Hz), 7.89 (AA'XX', 2H, *J*<sub>AX</sub> = 8.8 Hz, *J*<sub>AA'/XX'</sub> = 2.2 Hz). <sup>13</sup>C-NMR (CDCl<sub>3</sub>) δ (ppm): 28.71 (2C), 43.46, 55.50, 112.32, 115.73, 119.01, 129.30 (2C), 129.76, 129.82 (2C), 134.11, 137.36, 139.91, 159.83, 170.34, 200.53. HPLC analysis: retention time = 12.387 min; peak area, 97% (254 nm).

**(4-(4-Chlorobenzoyl)piperidin-1-yl)(2-methoxyphenyl)methanone (15c).** Orange solid; yield 36% from **21** and 2-methoxybenzoic acid; <sup>1</sup>H-NMR (CDCl<sub>3</sub>; asterisk denotes isomer peaks) δ (ppm): 1.70-2.05 (m, 4H), 2.97-3.20 (m, 2H), 3.40-3.50 (m, 1H), 3.57-3.65 (m, 1H), 3.84\* (s, 3H), 3.85 (s, 3H), 4.72-4.81 (m, 1H), 6.89-6.93 (m, 1H), 6.96-7.02 (m, 1H), 7.21-7.25 (m, 1H), 7.32-7.37 (m, 1H), 7.43-7.48 (m, 2H), 7.86-7.91 (m, 2H). <sup>13</sup>C-NMR (CDCl<sub>3</sub>; asterisk denotes isomer peaks) δ (ppm): 28.63, 28.70\*, 41.13\*, 41.23, 43.55, 43.63\*, 46.12\*, 46.74, 55.66, 55.74\*, 110.99\*, 111.08, 121.01\*, 121.15, 125.92, 126.03\*, 127.94, 128.05\*, 129.26 (2C), 129.81 (2C), 130.50\*, 130.54, 134.17, 139.82, 139.84\*, 155.44\*, 155.51, 167.87\*, 168.09, 200.61, 200.70\*. HPLC analysis: retention time = 12.219 min; peak area, 95% (254 nm).

**(4-(4-Chlorobenzoyl)piperidin-1-yl)(4-(trifluoromethoxy)phenyl)methanone (16a).** Orange solid; yield 54% from **21** and 4-(trifluoromethoxy)benzoic acid; <sup>1</sup>H-NMR (CDCl<sub>3</sub>) δ (ppm): 1.74-2.07 (m, 4H), 3.01-3.23 (bm, 2H), 3.46-3.55 (m, 1H), 3.74-3.95 (bm, 1H), 4.53-4.76 (bm, 1H), 7.24-

7.28 (m, 2H), 7.44-7.49 (m, 4H), 7.89 (AA'XX', 2H,  $J_{AX} = 8.7$  Hz,  $J_{AA'/XX'} = 2.0$  Hz).  $^{13}\text{C-NMR}$  ( $\text{CDCl}_3$ )  $\delta$  (ppm): 28.65 (2C), 43.28, 120.49 (q,  $J = 258.2$  Hz), 121.06 (2C), 128.87 (2C), 129.31 (2C), 129.81 (2C), 134.03, 134.60, 139.97, 150.17 (q,  $J = 1.3$  Hz), 169.28, 200.38. HPLC analysis: retention time = 13.405 min; peak area, 98% (254 nm).

**(4-(4-Chlorobenzoyl)piperidin-1-yl)(3-(trifluoromethoxy)phenyl)methanone (16b).** Orange solid; yield 47% from **21** and 3-(trifluoromethoxy)benzoic acid;  $^1\text{H-NMR}$  ( $\text{CDCl}_3$ )  $\delta$  (ppm): 1.74-2.10 (m, 4H), 3.00-3.25 (bm, 2H), 3.45-3.55 (m, 1H), 3.72-3.90 (bm, 1H), 4.58-4.73 (bm, 1H), 7.25-7.30 (m, 2H), 7.35 (d, 1H,  $J = 7.6$  Hz), 7.43-7.49 (m, 3H), 7.87-7.91 (m, 2H).  $^{13}\text{C-NMR}$  ( $\text{CDCl}_3$ )  $\delta$  (ppm): 28.60 (2C), 43.25, 119.73, 120.52 (q,  $J = 257.9$  Hz), 122.24, 125.37, 129.31 (2C), 129.81 (2C), 130.34, 134.03, 137.94, 139.98, 149.32 (q,  $J = 2.0$  Hz), 168.78, 200.34. HPLC analysis: retention time = 13.420 min; peak area, 97% (254 nm).

**(4-(4-Chlorobenzoyl)piperidin-1-yl)(2-(trifluoromethoxy)phenyl)methanone (16c).** Orange solid; yield 50% from **21** and 2-(trifluoromethoxy)benzoic acid;  $^1\text{H-NMR}$  ( $\text{CDCl}_3$ )  $\delta$  (ppm): 1.70-2.04 (m, 4H), 3.02-3.26 (m, 2H), 3.40-3.62 (m, 2H), 4.68-4.78 (m, 1H), 7.28-7.48 (m, 6H), 7.89 (AA'XX', 2H,  $J_{AX} = 8.6$  Hz,  $J_{AA'/XX'} = 2.1$  Hz).  $^{13}\text{C-NMR}$  ( $\text{CDCl}_3$ ; asterisk denotes isomer peaks)  $\delta$  (ppm): 28.36\*, 28.46, 28.52\*, 28.63, 41.19, 41.39\*, 43.17, 43.35\*, 46.17, 46.68\*, 120.55 (q,  $J = 258.6$  Hz), 120.61, 120.68\*, 127.30\*, 127.38, 128.75, 128.85\*, 129.30, 129.81 (4C), 130.80, 134.02, 134.07\*, 139.83\*, 139.97, 145.00, 165.62, 200.22\*, 200.47. HPLC analysis: retention time = 13.205 min; peak area, 97% (254 nm).

**(4-(4-Chlorobenzoyl)piperidin-1-yl)(4-hydroxyphenyl)methanone (17a).** Beige solid; yield 69% from **4**;  $^1\text{H-NMR}$  ( $\text{DMSO-}d_6$ )  $\delta$  (ppm): 1.43-1.55 (m, 2H), 1.76-1.87 (m, 2H), 2.99-3.16 (bm, 2H), 3.73 (tt, 1H,  $J = 11.1, 3.5$  Hz), 3.95-4.30 (bm, 2H), 6.77 (AA'XX', 2H,  $J_{AX} = 8.7$  Hz,  $J_{AA'/XX'} = 2.4$  Hz), 7.25 (AA'XX', 2H,  $J_{AX} = 8.7$  Hz,  $J_{AA'/XX'} = 2.4$  Hz), 7.61 (AA'XX', 2H,  $J_{AX} = 8.8$  Hz,  $J_{AA'/XX'} = 2.2$  Hz), 8.02 (AA'XX', 2H,  $J_{AX} = 8.8$  Hz,  $J_{AA'/XX'} = 2.3$  Hz), 9.82 (exchangeable bs, 1H).  $^{13}\text{C-NMR}$  ( $\text{DMSO-}d_6$ )  $\delta$  (ppm): 28.29 (2C), 42.49, 114.85 (2C), 126.37, 128.94 (2C), 128.95 (2C), 130.18 (2C),

134.12, 138.13, 158.58, 169.33, 200.93. HPLC analysis: retention time = 11.077 min; peak area, 99% (254 nm).

**(4-(4-Chlorobenzoyl)piperidin-1-yl)(3-hydroxyphenyl)methanone (17b).** White solid; yield 94% from **15b**;  $^1\text{H-NMR}$  (acetone- $d_6$ )  $\delta$  (ppm): 1.59-1.71 (m, 2H), 1.81-2.00 (bm, 2H), 2.90-3.30 (bm, 2H), 3.79 (tt, 1H,  $J = 11.3, 3.7$  Hz), 4.40-4.70 (bm, 2H), 6.85-6.92 (m, 3H), 7.23-7.28 (m, 1H), 7.57 (AA'XX', 2H,  $J_{AX} = 8.8$  Hz,  $J_{AA'/XX'} = 2.2$  Hz), 8.07 (AA'XX', 2H,  $J_{AX} = 8.8$  Hz,  $J_{AA'/XX'} = 2.3$  Hz), 8.58 (exchangeable bs, 1H).  $^{13}\text{C-NMR}$  (acetone- $d_6$ )  $\delta$  (ppm): 44.02, 114.62, 117.12, 118.71, 129.83 (2C), 130.40, 131.00 (2C), 135.55, 139.11, 139.59, 158.27, 170.14, 201.33. HPLC analysis: retention time = 11.262 min; peak area, 99% (254 nm).

**(4-(4-Chlorobenzoyl)piperidin-1-yl)(2-hydroxyphenyl)methanone (17c).** Grey solid; yield 76% from **15c**;  $^1\text{H-NMR}$  (acetone- $d_6$ )  $\delta$  (ppm): 1.66-1.78 (m, 2H), 1.92-2.00 (m, 2H), 3.17-3.28 (m, 2H), 3.81 (tt, 1H,  $J = 11.2, 3.7$  Hz), 4.22-4.35 (bm, 2H), 6.87-6.95 (m, 2H), 7.27-7.32 (m, 2H), 7.57 (AA'XX', 2H,  $J_{AX} = 8.7$  Hz,  $J_{AA'/XX'} = 2.2$  Hz), 8.07 (AA'XX', 2H,  $J_{AX} = 8.7$  Hz,  $J_{AA'/XX'} = 2.2$  Hz), 9.33 (exchangeable s, 1H).  $^{13}\text{C-NMR}$  (acetone- $d_6$ )  $\delta$  (ppm): 43.95, 117.48, 119.93, 122.03, 129.35, 129.84 (2C), 131.01, 132.10 (2C), 135.56, 139.60, 157.19, 169.72, 201.31. HPLC analysis: retention time = 11.492 min; peak area, 99% (254 nm).

**(1-(4-Aminobenzoyl)piperidin-4-yl)(4-chlorophenyl)methanone (18a).** Beige solid; yield 77% from **31**;  $^1\text{H-NMR}$  (acetone- $d_6$ )  $\delta$  (ppm): 1.58-1.70 (m, 2H), 1.86-1.94 (m, 2H), 3.06-3.16 (m, 2H), 3.76 (tt, 1H,  $J = 11.3, 3.8$  Hz), 4.22-4.32 (bm, 1H), 4.93-5.03 (bm, 1H), 6.67 (AA'XX', 2H,  $J_{AX} = 8.6$  Hz,  $J_{AA'/XX'} = 2.3$  Hz), 7.21 (AA'XX', 2H,  $J_{AX} = 8.6$  Hz,  $J_{AA'/XX'} = 2.2$  Hz), 7.57 (AA'XX', 2H,  $J_{AX} = 8.8$  Hz,  $J_{AA'/XX'} = 2.3$  Hz), 8.06 (AA'XX', 2H,  $J_{AX} = 8.8$  Hz,  $J_{AA'/XX'} = 2.2$  Hz).  $^{13}\text{C-NMR}$  (acetone- $d_6$ )  $\delta$  (ppm): 44.17, 114.00 (2C), 119.92, 129.02, 129.79 (2C), 130.03 (2C), 130.98 (2C), 135.55, 139.51, 171.15, 201.40. HPLC analysis: retention time = 11.037 min; peak area, 98% (254 nm).

**(1-(3-Aminobenzoyl)piperidin-4-yl)(4-chlorophenyl)methanone (18b).** Beige solid; yield 89% from **30**;  $^1\text{H-NMR}$  (acetone- $d_6$ )  $\delta$  (ppm): 1.57-1.68 (m, 2H), 1.83-1.95 (bm, 2H), 2.90-3.30 (bm, 2H), 3.78 (tt, 1H,  $J = 11.2, 3.7$  Hz), 4.76-4.82 (bm, 2H), 6.60 (dt, 1H,  $J = 7.5, 1.3$  Hz), 6.69-6.73 (m, 2H),



7.09 (dd, 1H,  $J = 8.7, 7.5$  Hz), 7.57 (AA'XX', 2H,  $J_{AX} = 8.8$  Hz,  $J_{AA'/XX'} = 2.3$  Hz), 8.06 (AA'XX', 2H,  $J_{AX} = 8.8$  Hz,  $J_{AA'/XX'} = 2.2$  Hz).  $^{13}\text{C}$ -NMR (acetone- $d_6$ )  $\delta$  (ppm): 44.08, 113.35, 115.69, 115.86, 129.77, 129.82 (2C), 130.99 (2C), 135.55, 138.56, 139.57, 149.44, 170.83, 201.37. HPLC analysis: retention time = 11.188 min; peak area, 99% (254 nm).

**(1-(2-Aminobenzoyl)piperidin-4-yl)(4-chlorophenyl)methanone (18c)**. Orange solid; yield 44% from **21** and anthranilic acid;  $^1\text{H}$ -NMR (acetone- $d_6$ )  $\delta$  (ppm): 1.62-1.73 (m, 2H), 1.88-1.97 (m, 2H), 3.10-3.21 (m, 2H), 3.78 (tt, 1H,  $J = 11.3, 3.7$  Hz), 4.14-4.32 (bm, 1H), 4.87-4.95 (bm, 1H), 6.62 (td, 1H,  $J = 7.4, 1.0$  Hz), 6.78 (dd, 1H,  $J = 8.1, 0.7$  Hz), 7.07-7.14 (m, 2H), 7.57 (AA'XX', 2H,  $J_{AX} = 8.8$  Hz,  $J_{AA'/XX'} = 2.2$  Hz), 8.06 (AA'XX', 2H,  $J_{AX} = 8.8$  Hz,  $J_{AA'/XX'} = 2.3$  Hz).  $^{13}\text{C}$ -NMR (acetone- $d_6$ )  $\delta$  (ppm): 44.06, 116.84, 116.94, 120.83, 128.61, 129.79, 129.80 (2C), 130.98 (2C), 135.53, 139.54, 147.44, 170.21, 201.32. HPLC analysis: retention time = 11.795 min; peak area, 95% (254 nm).

**(4-(4-Chlorobenzoyl)piperidin-1-yl)(4-nitrophenyl)methanone (19a)**. Yellow solid; yield 48% from **21** and 4-nitrobenzoic acid;  $^1\text{H}$ -NMR ( $\text{CDCl}_3$ )  $\delta$  (ppm): 1.74-2.10 (m, 4H), 3.04-3.28 (bm, 2H), 3.49-3.59 (m, 1H), 3.66-3.80 (bm, 1H), 4.61-4.73 (bm, 1H), 7.47 (AA'XX', 2H,  $J_{AX} = 8.8$  Hz,  $J_{AA'/XX'} = 2.2$  Hz), 7.59 (AA'XX', 2H,  $J_{AX} = 8.9$  Hz,  $J_{AA'/XX'} = 2.1$  Hz), 7.89 (AA'XX', 2H,  $J_{AX} = 8.8$  Hz,  $J_{AA'/XX'} = 2.2$  Hz), 8.29 (AA'XX', 2H,  $J_{AX} = 8.8$  Hz,  $J_{AA'/XX'} = 2.1$  Hz).  $^{13}\text{C}$ -NMR ( $\text{CDCl}_3$ )  $\delta$  (ppm): 28.61 (2C), 43.10, 124.05 (2C), 128.05 (2C), 129.35 (2C), 129.80 (2C), 134.07, 140.08, 142.25, 148.65, 168.19, 200.16. HPLC analysis: retention time = 12.470 min; peak area, 99% (254 nm).

**(4-(4-Chlorobenzoyl)piperidin-1-yl)(3-nitrophenyl)methanone (19b)**. Orange solid; yield 55% from **21** and 3-nitrobenzoic acid;  $^1\text{H}$ -NMR ( $\text{CDCl}_3$ )  $\delta$  (ppm): 1.77-2.10 (m, 4H), 3.08-3.30 (bm, 2H), 3.49-3.58 (m, 1H), 3.72-3.85 (bm, 1H), 4.58-4.73 (bm, 1H), 7.47 (AA'XX', 2H,  $J_{AX} = 8.7$  Hz,  $J_{AA'/XX'} = 2.2$  Hz), 7.63 (td, 1H,  $J = 7.6, 1.3$  Hz), 7.77 (dt, 1H,  $J = 7.7, 1.3$  Hz), 7.89 (AA'XX', 2H,  $J_{AX} = 8.7$  Hz,  $J_{AA'/XX'} = 2.2$  Hz), 8.27-8.31 (m, 2H).  $^{13}\text{C}$ -NMR ( $\text{CDCl}_3$ )  $\delta$  (ppm): 28.55 (2C), 43.03, 122.22, 124.62, 129.31 (2C), 129.79 (2C), 129.96, 133.03, 133.94, 137.60, 139.99, 148.21, 167.84, 200.20. HPLC analysis: retention time = 12.445 min; peak area, 96% (254 nm).

**(4-(4-Chlorobenzoyl)piperidin-1-yl)(2-nitrophenyl)methanone (19c).** Light-yellow solid; yield 54% from **21** and 2-nitrobenzoic acid;  $^1\text{H-NMR}$  ( $\text{CDCl}_3$ )  $\delta$  (ppm): 1.71-1.86 (bm, 3H), 2.02-2.13 (bm, 1H), 3.10-3.25 (bm, 2H), 3.42-3.56 (bm, 2H), 4.57-4.76 (bm, 1H), 7.36-7.48 (m, 3H), 7.57 (td, 1H,  $J = 8.5, 1.3$  Hz), 7.68-7.75 (m, 1H), 7.84-7.91 (m, 2H), 8.20 (d, 1H,  $J = 8.2$  Hz).  $^{13}\text{C-NMR}$  ( $\text{CDCl}_3$ )  $\delta$  (ppm): 27.96, 28.38, 41.27, 43.01, 46.01, 124.95, 128.12, 129.33, 129.83 (3C), 129.96, 133.16, 134.05, 134.78, 140.00, 145.30, 166.90, 200.58. HPLC analysis: retention time = 12.240 min; peak area, 97% (254 nm).

**(1-Benzoylpiperidin-4-yl)(4-chlorophenyl)methanone (20).** Light-yellow solid; yield 61% from **21** and benzoic acid;  $^1\text{H-NMR}$  ( $\text{CDCl}_3$ )  $\delta$  (ppm): 1.70-2.00 (m, 4H), 2.97-3.23 (bm, 2H), 3.45-3.53 (m, 1H), 3.80-3.95 (bm, 1H), 4.57-4.70 (bm, 1H), 7.41 (s, 5H), 7.46 (AA'XX', 2H,  $J_{AX} = 8.6$  Hz,  $J_{AA'XX'} = 2.1$  Hz), 7.89 (AA'XX', 2H,  $J_{AX} = 8.6$  Hz,  $J_{AA'XX'} = 2.1$  Hz).  $^{13}\text{C-NMR}$  ( $\text{CDCl}_3$ )  $\delta$  (ppm): 28.71 (2C), 43.47, 127.00 (2C), 128.64 (2C), 129.30, 129.82 (4C), 134.11, 136.09, 139.92, 170.62, 200.52. HPLC analysis: retention time = 12.259 min; peak area, 98% (254 nm).

**(4-([1,1'-Biphenyl]-4-carbonyl)piperidin-1-yl)(3-hydroxyphenyl)methanone (43).** White solid; yield 82% from **44**;  $^1\text{H-NMR}$  ( $\text{DMSO-}d_6$ )  $\delta$  (ppm): 1.46-1.59 (m, 2H), 1.72-1.98 (bm, 2H), 2.90-3.10 (bm, 1H), 3.10-3.30 (bm, 1H), 3.60-3.75 (bm, 1H), 3.80 (tt, 1H,  $J = 11.2, 3.4$  Hz), 4.40-4.57 (bm, 1H), 6.74-6.80 (m, 2H), 6.82 (ddd, 1H,  $J = 8.1, 2.5, 1.0$  Hz), 7.23 (t, 1H,  $J = 7.7$  Hz), 7.44 (tt, 1H,  $J = 7.3, 1.5$  Hz), 7.48-7.54 (m, 2H), 7.73-7.78 (m, 2H), 7.82-7.87 (m, 2H), 8.08-8.12 (m, 2H), 9.67 (exchangeable s, 1H), 9.82 (exchangeable bs, 1H).  $^{13}\text{C-NMR}$  ( $\text{DMSO-}d_6$ )  $\delta$  (ppm): 42.43, 113.40, 116.31, 117.09, 127.03 (2C), 127.07 (2C), 128.44, 129.04 (2C), 129.12 (2C), 129.62, 134.24, 137.51, 138.88, 144.66, 157.29, 168.95, 201.46. HPLC analysis: retention time = 12.153 min; peak area, 99% (254 nm).

**Docking Calculations.** The crystal structure of *hMAGL* (pdb code 3PE6<sup>20</sup>) was taken from the Protein Data Bank.<sup>29</sup> After adding hydrogen atoms the protein complexed with its reference inhibitor was minimized using Amber14 software<sup>30</sup> and ff14SB force field at 300 K. The complex was placed in a rectangular parallelepiped water box, an explicit solvent model for water, TIP3P, was used and

the complex was solvated with a 10 Å water cap. Sodium ions were added as counter ions to neutralize the system. Two steps of minimization were then carried out; in the first stage, we kept the protein fixed with a position restraint of 500 kcal/mol Å<sup>2</sup> and we solely minimized the positions of the water molecules. In the second stage, we minimized the entire system through 5000 steps of steepest descent followed by conjugate gradient (CG) until a convergence of 0.05 kcal/Å•mol. The ligands were built using Maestro<sup>31</sup> and were minimized by means of Macromodel<sup>32</sup> in a water environment using the CG method until a convergence value of 0.05 kcal/Å mol, using the MMFFs force field and a distance-dependent dielectric constant of 1.0. Automated docking was carried out by means of the AUTODOCK 4.0 program;<sup>33</sup> Autodock Tools<sup>34</sup> was used in order to identify the torsion angles in the ligands, add the solvent model and assign the Kollman atomic charges to the protein. The ligand charge was calculated using the Gasteiger method. The regions of interest used by Autodock were defined by considering the ZYH reference inhibitor as the central group; in particular, a grid of 82, 40, and 30 points in the x, y, and z directions was constructed centered on the center of the mass of this compound. A grid spacing of 0.375 Å and a distance-dependent function of the dielectric constant were used for the energetic map calculations. Using the Lamarckian Genetic Algorithm, the docked compounds were subjected to 100 runs of the Autodock search, using 500000 steps of energy evaluation and the default values of the other parameters. Cluster analysis was performed on the results using an RMS tolerance of 2.0 Å.

**MD Simulations.** All simulations were performed using AMBER, version 14.<sup>30</sup> MD simulations were carried out using the ff14SB force field at 300 K. The complex was placed in a rectangular parallelepiped water box. An explicit solvent model for water, TIP3P, was used, and the complex was solvated with a 20 Å water cap. Sodium ions were added as counterions to neutralize the system. Prior to MD simulations, two steps of minimization were carried out using the same procedure described above. Particle Mesh Ewald (PME) electrostatics and periodic boundary conditions were used in the simulation.<sup>35</sup> The MD trajectory was run using the minimized structure as the starting conformation. The time step of the simulations was 2.0 fs with a cutoff of 10 Å for the nonbonded

interaction, and SHAKE was employed to keep all bonds involving hydrogen atoms rigid. Constant-volume periodic boundary MD was carried out for 1.0 ns, during which the temperature was raised from 0 to 300 K. Then 50 ns of constant pressure periodic boundary MD was carried out at 300 K using the Langevin thermostat to maintain constant the temperature of our system. All the  $\alpha$  carbons of the protein were blocked with a harmonic force constant of 10 kcal/mol $\cdot\text{\AA}^2$ . General Amber force field (GAFF) parameters were assigned to the ligand, while partial charges were calculated using the AM1-BCC method as implemented in the Antechamber suite of AMBER 14. The final structure of the complex was obtained as the average of the last 50.0 ns of MD minimized by the CG method until a convergence of 0.05 kcal/mol $\cdot\text{\AA}^2$ . The average structure was obtained using the Cpptraj program<sup>36</sup> implemented in AMBER 14.

**MAGL inhibition assay.** Human recombinant MAGL, **1**, **2** and 4-NPA substrate were from Cayman Chemical. The  $IC_{50}$  values for compounds were generated in 96-well microtiter plates. The MAGL reaction was conducted at room temperature at a final volume of 200  $\mu\text{L}$  in 10 mM Tris buffer, pH 7.2, containing 1 mM EDTA and BSA 0.1 mg/ml. A total of 150  $\mu\text{L}$  of 4-NPA 133.3  $\mu\text{M}$  was added to 10  $\mu\text{L}$  of DMSO containing the appropriate amount of compound. The reaction was initiated by the addition of 40  $\mu\text{L}$  of MAGL (11 ng/well) in such a way that the assay was linear over 30 min. The final concentration of the analyzed compounds ranged for **1** and **2** from 10 to 0.00001  $\mu\text{M}$  and for the other compounds from 200 to 0.0128  $\mu\text{M}$ . After the reaction had proceeded for 30 min, absorbance values were then measured by using a Victor X3 Microplates Reader (PerkinElmer®) at 405 nm.<sup>5</sup> Two reactions were also run: one reaction containing no compounds and the second one containing neither inhibitor nor enzyme.  $IC_{50}$  values were derived from experimental data using the Sigmoidal dose–response fitting of GraphPad Prism software. To remove possible false positive results, for each compound concentration a blank analysis was carried out, and the final absorbance results were obtained deducting the absorbance produced by the presence of all the components except MAGL in the same conditions. In the enzyme kinetics experiments, compound was tested in the presence of scalar concentrations of 4-NPA. It was added in scalar amounts (concentration range = 1–10  $\mu\text{M}$ ) to

a reaction mixture containing Tris buffer and scalar concentrations of 4-NPA (15–1400  $\mu\text{M}$ ). Finally, MAGL solution was added (11 ng/well). The MAGL activity was measured by recording the increase in 4-nitrophenol absorbance using the Victor X3 Microplates Reader (PerkinElmer®). The experimental data were analyzed by non-linear regression analysis with GraphPad Prism software, using a second order polynomial regression analysis, and by applying the mixed-model inhibition fit.

**FAAH inhibition assay.** The  $\text{IC}_{50}$  values for compounds were generated in 96-well microtiter plates. The FAAH reaction was conducted at room temperature at a final volume of 200  $\mu\text{L}$  in 125 mM Tris buffer, pH 9.0, containing 1 mM EDTA and in the presence of BSA 0.1 mg/ml. A total of 150  $\mu\text{L}$  of AMC arachidonoylamide 13.3  $\mu\text{M}$  (final concentration = 10  $\mu\text{M}$ ) was added to 10  $\mu\text{L}$  of DMSO containing the appropriate amount of compound. The reaction was initiated by the addition of 40  $\mu\text{L}$  of FAAH (0.9  $\mu\text{g}/\text{well}$ ) in such a way that the assay was linear over 30 min. The final concentration of the analyzed compounds ranged for from 200 to 0.0128  $\mu\text{M}$ . After the reaction had proceeded for 30 min, fluorescence values were then measured by using a Victor X3 PerkinElmer instrument at an excitation wavelength of 340 nm and an emission of 460 nm. Two reactions were also run: one reaction containing no compounds and the second one containing neither inhibitor nor enzyme.  $\text{IC}_{50}$  values were derived from experimental data using the Sigmoidal dose–response fitting of GraphPad Prism software. To remove possible false positive results, for each compound concentration a blank analysis was carried out, and the final fluorescence results were obtained deducting the fluorescence produced by the presence of all the components except FAAH in the same conditions.

**Cell viability assay.** OVSAHO, OVCAR3, COV318, CAOV3 and MRC5 (from ATCC) were maintained at 37 °C in a humidified atmosphere containing 5%  $\text{CO}_2$  accordingly to the supplier. Normal ( $1.5 \times 10^4$ ) and tumor ( $5 \times 10^2$ ) cells were plated in 96-well culture plates. The day after seeding, vehicle or compounds were added at different concentrations to the medium. Compounds were added to the cell culture at a concentration ranging from 200 to 0.02  $\mu\text{M}$ . Cell viability was measured after 96 h according to the supplier (Promega, G7571) with a Tecan F200 instrument.  $\text{IC}_{50}$

values were calculated from logistical dose response curves. Averages were obtained from three independent experiments, and error bars are standard deviations (n = 3).

**Western blot analysis.** Cancer cells were pelleted and resuspended into RIPA buffer supplemented 3 with a protease inhibitor mixture (Complete-EDTA, Roche, Switzerland) for protein extraction.<sup>37</sup> Fifty µg of proteins were run in 8% denaturing polyacrylamide gel. After electrophoresis, the proteins were transferred on nitrocellulose membrane (Whatman International Ltd, UK). The membranes were blocked with 5% (w/v) skim milk in Tris-buffered saline Tween 20 solution (TBS-T) and incubated overnight with primary antibodies (Vinculin (sc-7649), 1:1000 from Santa Cruz, CA, US; MAGL (Ab24701) 1:1000 from Abcam, Cambridge, UK). After washing, membranes were incubated for 1 h with secondary antibodies in 5% milk TBS-T at RT, developed with enhanced chemiluminescence (ECL) solution and visualized with ChemiDoc Imager instrument (Bio-Rad Laboratories, CA, US).<sup>38</sup>

## SUPPORTING INFORMATION

Clustering analysis, docking results of compound **17c** and **17a**, MD simulation analysis of **17b**, <sup>1</sup>H-NMR spectra of compound **12c**, interference analysis for compound **17b**, effect of DTT on the **17b** inhibition properties, cell growth inhibitory activities of compounds **17b**, **2** and **3**, IC<sub>50</sub> plot of MAGL inhibition of compound **43**, analytical data on intermediate compounds, HPLC chromatograms and NMR spectra of the final compounds. This material is available free of charge via the Internet at <http://pubs.acs.org>.

## CORRESPONDING AUTHOR INFORMATION

Corresponding author phone: +39 0502219595; e-mail: [tiziano.tuccinardi@unipi.it](mailto:tiziano.tuccinardi@unipi.it)

## ACKNOWLEDGMENTS

This work was supported by the University of Pisa under the PRA program (project PRA\_2016\_27 and PRA\_2016\_59).

## ABBREVIATIONS USED

MAGL, monoacylglycerol lipase; AEA, anandamide; 2-AG, 2-arachidonoylglycerol; EAE, experimental allergic encephalomyelitis; FAAH, fatty acid amide hydrolase; PAINS, pan assay interference compounds; 4-NPA, 4-nitrophenylacetate; 4-NP, 4-nitrophenol; CG, conjugate gradient; PME, Particle Mesh Ewald; GAFF, general Amber force field; ECL, enhanced chemiluminescence.

## REFERENCES

1. Pacher, P.; Batkai, S.; Kunos, G. The endocannabinoid system as an emerging target of pharmacotherapy. *Pharmacol. Rev.* **2006**, *58*, 389-462.
2. Di Marzo, V. The endocannabinoid system: its general strategy of action, tools for its pharmacological manipulation and potential therapeutic exploitation. *Pharmacol. Res.* **2009**, *60*, 77-84.
3. Di Iorio, G.; Lupi, M.; Sarchione, F.; Matarazzo, I.; Santacrose, R.; Petruccioli, F.; Martinotti, G.; Di Giannantonio, M. The endocannabinoid system: a putative role in neurodegenerative diseases. *Int. J. High Risk Behav. Addict.* **2013**, *2*, 100-106.
4. Scavini, L.; Piomelli, D.; Mor, M. Monoglyceride lipase: structure and inhibitors. *Chem. Phys. Lipids* **2016**, *197*, 13-24.
5. Muccioli, G. G.; Labar, G.; Lambert, D. M. CAY10499, a novel monoglyceride lipase inhibitor evidenced by an expeditious MGL assay. *Chembiochem* **2008**, *9*, 2704-2710.
6. Zvonok, N.; Pandarinathan, L.; Williams, J.; Johnston, M.; Karageorgos, I.; Janero, D. R.; Krishnan, S. C.; Makriyannis, A. Covalent inhibitors of human monoacylglycerol lipase: ligand-assisted characterization of the catalytic site by mass spectrometry and mutational analysis. *Chem. Biol.* **2008**, *15*, 854-862.

7. King, A. R.; Lodola, A.; Carmi, C.; Fu, J.; Mor, M.; Piomelli, D. A critical cysteine residue in monoacylglycerol lipase is targeted by a new class of isothiazolinone-based enzyme inhibitors. *Br. J. Pharmacol.* **2009**, *157*, 974-983.
8. Long, J. Z.; Li, W.; Booker, L.; Burston, J. J.; Kinsey, S. G.; Schlosburg, J. E.; Pavon, F. J.; Serrano, A. M.; Selley, D. E.; Parsons, L. H.; Lichtman, A. H.; Cravatt, B. F. Selective blockade of 2-arachidonoylglycerol hydrolysis produces cannabinoid behavioral effects. *Nat. Chem. Biol.* **2009**, *5*, 37-44.
9. Matuszak, N.; Muccioli, G. G.; Labar, G.; Lambert, D. M. Synthesis and in vitro evaluation of N-substituted maleimide derivatives as selective monoglyceride lipase inhibitors. *J. Med. Chem.* **2009**, *52*, 7410-7420.
10. Kapanda, C. N.; Masquelier, J.; Labar, G.; Muccioli, G. G.; Poupaert, J. H.; Lambert, D. M. Synthesis and pharmacological evaluation of 2,4-dinitroaryldithiocarbamate derivatives as novel monoacylglycerol lipase inhibitors. *J. Med. Chem.* **2012**, *55*, 5774-5783.
11. Labar, G.; Wouters, J.; Lambert, D. M. A review on the monoacylglycerol lipase: at the interface between fat and endocannabinoid signalling. *Curr. Med. Chem.* **2010**, *17*, 2588-2607.
12. Schlosburg, J. E.; Blankman, J. L.; Long, J. Z.; Nomura, D. K.; Pan, B.; Kinsey, S. G.; Nguyen, P. T.; Ramesh, D.; Booker, L.; Burston, J. J.; Thomas, E. A.; Selley, D. E.; Sim-Selley, L. J.; Liu, Q. S.; Lichtman, A. H.; Cravatt, B. F. Chronic monoacylglycerol lipase blockade causes functional antagonism of the endocannabinoid system. *Nat. Neurosci.* **2010**, *13*, 1113-1119.
13. King, A. R.; Dotsey, E. Y.; Lodola, A.; Jung, K. M.; Ghomian, A.; Qiu, Y.; Fu, J.; Mor, M.; Piomelli, D. Discovery of potent and reversible monoacylglycerol lipase inhibitors. *Chem. Biol.* **2009**, *16*, 1045-1052.
14. Petronelli, A.; Pannitteri, G.; Testa, U. Triterpenoids as new promising anticancer drugs. *Anticancer Drugs* **2009**, *20*, 880-892.



15. Wang, L.; Wang, G.; Yang, D.; Guo, X.; Xu, Y.; Feng, B.; Kang, J. Euphol arrests breast cancer cells at the G1 phase through the modulation of cyclin D1, p21 and p27 expression. *Mol. Med. Rep.* **2013**, *8*, 1279-1285.
16. Hernandez-Torres, G.; Cipriano, M.; Heden, E.; Bjorklund, E.; Canales, A.; Zian, D.; Feliu, A.; Mecha, M.; Guaza, C.; Fowler, C. J.; Ortega-Gutierrez, S.; Lopez-Rodriguez, M. L. A reversible and selective inhibitor of monoacylglycerol lipase ameliorates multiple sclerosis. *Angew. Chem., Int. Ed. Engl* **2014**, *53*, 13765-13770.
17. Tuccinardi, T.; Granchi, C.; Rizzolio, F.; Caligiuri, I.; Battistello, V.; Toffoli, G.; Minutolo, F.; Macchia, M.; Martinelli, A. Identification and characterization of a new reversible MAGL inhibitor. *Bioorg. Med. Chem.* **2014**, *22*, 3285-3291.
18. Labar, G.; Bauvois, C.; Borel, F.; Ferrer, J. L.; Wouters, J.; Lambert, D. M. Crystal structure of the human monoacylglycerol lipase, a key actor in endocannabinoid signaling. *Chembiochem* **2010**, *11*, 218-227.
19. Bertrand, T.; Auge, F.; Houtmann, J.; Rak, A.; Vallee, F.; Mikol, V.; Berne, P. F.; Michot, N.; Cheuret, D.; Hoornaert, C.; Mathieu, M. Structural basis for human monoglyceride lipase inhibition. *J. Mol. Biol.* **2010**, *396*, 663-673.
20. Schalk-Hihi, C.; Schubert, C.; Alexander, R.; Bayoumy, S.; Clemente, J. C.; Deckman, I.; DesJarlais, R. L.; Dzordzorme, K. C.; Flores, C. M.; Grasberger, B.; Kranz, J. K.; Lewandowski, F.; Liu, L.; Ma, H.; Maguire, D.; Macielag, M. J.; McDonnell, M. E.; Mezzasalma Haarlander, T.; Miller, R.; Milligan, C.; Reynolds, C.; Kuo, L. C. Crystal structure of a soluble form of human monoglyceride lipase in complex with an inhibitor at 1.35 Å resolution. *Protein Sci.* **2011**, *20*, 670-683.
21. Griebel, G.; Pichat, P.; Beeske, S.; Leroy, T.; Redon, N.; Jacquet, A.; Francon, D.; Bert, L.; Even, L.; Lopez-Grancha, M.; Tolstykh, T.; Sun, F.; Yu, Q.; Brittain, S.; Arlt, H.; He, T.; Zhang, B.; Wiederschain, D.; Bertrand, T.; Houtmann, J.; Rak, A.; Vallee, F.; Michot, N.; Auge, F.; Menet, V.; Bergis, O. E.; George, P.; Avenet, P.; Mikol, V.; Didier, M.; Escoubet, J. Selective blockade of the

hydrolysis of the endocannabinoid 2-arachidonoylglycerol impairs learning and memory performance while producing antinociceptive activity in rodents. *Sci. Rep.* **2015**, *5*, 7642.

22. Wang, X.; Sarris, K.; Kage, K.; Zhang, D.; Brown, S. P.; Kolasa, T.; Surowy, C.; El Kouhen, O. F.; Muchmore, S. W.; Brioni, J. D.; Stewart, A. O. Synthesis and evaluation of benzothiazole-based analogues as novel, potent, and selective fatty acid amide hydrolase inhibitors. *J. Med. Chem.* **2009**, *52*, 170-180.

23. Nomura, D. K.; Long, J. Z.; Niessen, S.; Hoover, H. S.; Ng, S. W.; Cravatt, B. F. Monoacylglycerol lipase regulates a fatty acid network that promotes cancer pathogenesis. *Cell* **2010**, *140*, 49-61.

24. Baell, J. B.; Holloway, G. A. New substructure filters for removal of pan assay interference compounds (PAINS) from screening libraries and for their exclusion in bioassays. *J. Med. Chem.* **2010**, *53*, 2719-2740.

25. Shoichet, B. K. Screening in a spirit haunted world. *Drug Discovery Today* **2006**, *11*, 607-615.

26. Dahlin, J. L.; Nissink, J. W.; Strasser, J. M.; Francis, S.; Higgins, L.; Zhou, H.; Zhang, Z.; Walters, M. A. PAINS in the assay: chemical mechanisms of assay interference and promiscuous enzymatic inhibition observed during a sulfhydryl-scavenging HTS. *J. Med. Chem.* **2015**, *58*, 2091-2113.

27. Dahlin, J. L.; Walters, M. A. How to triage PAINS-full research. *Assay Drug Dev. Technol.* **2016**, *14*, 168-174.

28. Del Carlo, S.; Manera, C.; Chicca, A.; Arena, C.; Bertini, S.; Bungalassi, S.; Tampucci, S.; Gertsch, J.; Macchia, M.; Saccomanni, G. Development of an HPLC/UV assay for the evaluation of inhibitors of human recombinant monoacylglycerol lipase. *J. Pharm. Biomed. Anal.* **2015**, *108*, 113-121.

29. Berman, H. M.; Westbrook, J.; Feng, Z.; Gilliland, G.; Bhat, T. N.; Weissig, H.; Shindyalov, I. N.; Bourne, P. E. The protein data bank. *Nucleic Acids Res.* **2000**, *28*, 235-242.

30. Case, D. A.; Berryman, J. T.; Betz, R. M.; Cerutti, D. S.; III, T. E. C.; Darden, T. A.; Duke, R. E.; Giese, T. J.; Gohlke, H.; Goetz, A. W.; Homeyer, N.; Izadi, S.; Janowski, P.; Kaus, J.; Kovalenko, A.; Lee, T. S.; LeGrand, S.; Li, P.; Luchko, T.; Luo, R.; Madej, B.; Merz, K. M.; Monard, G.; Needham, P.; Nguyen, H.; Nguyen, H. T.; Omelyan, I.; Onufriev, A.; Roe, D. R.; Roitberg, A.; Salomon-Ferrer, R.; Simmerling, C. L.; Smith, W.; Swails, J.; Walker, R. C.; Wang, J.; Wolf, R. M.; Wu, X.; York, D. M.; Kollman, P. A. *AMBER*, version 14. University of California: San Francisco, CA, 2015.
31. *Maestro*, version 9.0. Schrödinger Inc: Portland, OR, 2009.
32. *Macromodel*, version 9.7. Schrödinger Inc: Portland, OR, 2009.
33. Morris, G. M.; Goodsell, D. S.; Halliday, R. S.; Huey, R.; Hart, W. E.; Belew, R. K.; Olson, A. J. Automated docking using a lamarckian genetic algorithm and an empirical binding free energy function. *J. Comput. Chem.* **1998**, *19*, 1639-1662.
34. Morris, G. M.; Huey, R.; Lindstrom, W.; Sanner, M. F.; Belew, R. K.; Goodsell, D. S.; Olson, A. J. AutoDock4 and AutoDockTools4: automated docking with selective receptor flexibility. *J. Comput. Chem.* **2009**, *30*, 2785-2791.
35. York, D. M.; Darden, T. A.; Pedersen, L. G. The effect of long-range electrostatic interactions in simulations of macromolecular crystals - a comparison of the ewald and truncated list methods. *J. Chem. Phys.* **1993**, *99*, 8345-8348.
36. Roe, D. R.; Cheatham, T. E., 3rd. PTRAJ and CPPTRAJ: software for processing and analysis of molecular dynamics trajectory data. *J. Chem. Theory Comput.* **2013**, *9*, 3084-3095.
37. Hadla, M.; Palazzolo, S.; Corona, G.; Caligiuri, I.; Canzonieri, V.; Toffoli, G.; Rizzolio, F. Exosomes increase the therapeutic index of doxorubicin in breast and ovarian cancer mouse models. *Nanomedicine* **2016**, *11*, 2431-2441.
38. Roberti, A.; Rizzolio, F.; Lucchetti, C.; de Leval, L.; Giordano, A. Ubiquitin-mediated protein degradation and methylation-induced gene silencing cooperate in the inactivation of the INK4/ARF locus in Burkitt lymphoma cell lines. *Cell Cycle* **2011**, *10*, 127-134.